MAGNETOM Flash

The Magazine of MRI

SCMR Issue 1/2013
Not for distribution in the USA

SIEMENS

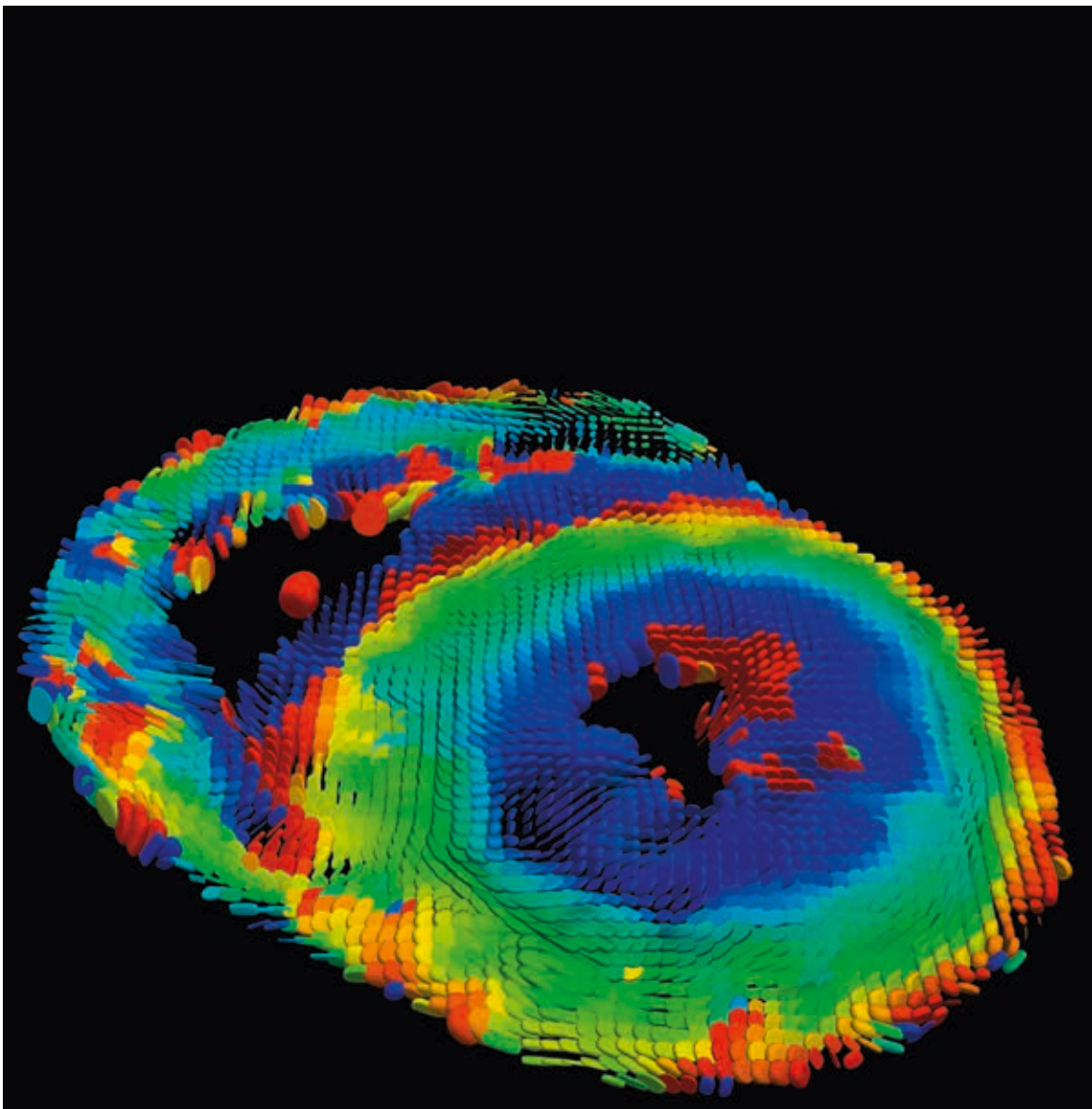

Diffusion Tensor Imaging in HCM

51

SCMR recommended protocols now available for Cardiac Dot Engine

To aid standardization of CMR, the Society for Cardiovascular Magnetic Resonance (SCMR) released CMR exam protocol recommendations for the most frequent CMR procedures. In a collaborational effort Siemens Healthcare and the SCMR prepared clinically optimized exam protocols in accordance to the SCMR recommendations for 3T MAGNETOM Skyra and 1.5T MAGNETOM Aera, with software version *syngo* MR D11.

The following SCMR Cardiac Dot protocols are available:

- Acute Infarct Dot
- Adenosine Stress Dot
- Aorta Dot
- Arrhythmic RV Myopathy Dot
- Chronic Ischemia Dot
- Coronaries Dot
- Mass & Thrombus Dot
- Nonischemic Myopathy Dot
- Pericardium Dot
- Peripheral MRA Dot
- Pulmonary Vein Dot
- Valves Dot
- Pediatric Teen Dot
- Pediatric Child Dot
- Pediatric Infant Dot
- Library Cardiac Shim
- Library TuneUp Shim

Please contact your Siemens Application Specialist for the .edx files of these protocols.

Acknowledgement: We would like to thank all SCMR members who were on the guidelines committee Christopher M. Kramer *(University of Virginia, Charlottesville, VA, USA);* Jörg Barkhausen *(University Hospital, Lübeck, Germany);* Scott D. Flamm *(Cleveland Clinic, Cleveland,OH, USA);* Raymond J. Kim *(Duke University Medical Center, Durham, NC, USA);* Eike Nagel *(King's College, London, UK)* as well as Gary R. McNeal *(Senior CMR Application Specialist; Siemens Healthcare, USA)* for their tremendous efforts and support.

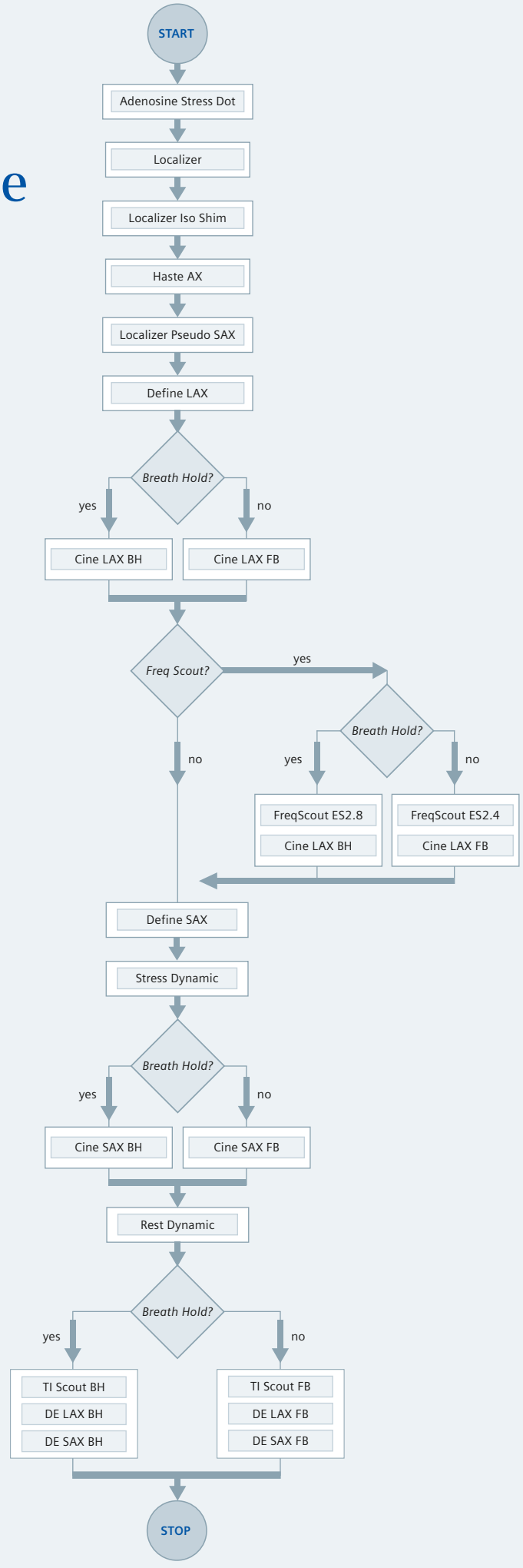

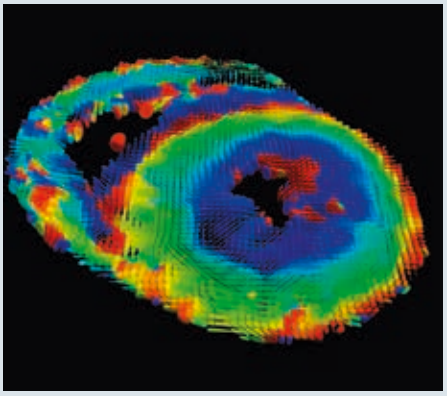

Cover image

Courtesy of Professor Dudley Pennell (*Royal Brompton Hospital, London, UK*)

In-vivo diffusion tensor imaging in the basal short-axis plane in a patient with hypertrophic cardiomyopathy (HCM).

Acquisition used a diffusion-weighted stimulated-echo single-shot echo-planar-imaging sequence during multiple breath-holds. The tensor is represented by superquadric glyphs, colour coded according to the helix angle of the main eigenvector (myocyte orientation): blue right-handed, green circumferential, red left-handed.

References

1 Nielles-Vallespin S, Mekkaoui C, Gatehouse P, Reese TG, Keegan J, Ferreira PF, Collins S, Speier P, Feiweier T, de Silva R, Jackowski MP, Pennell DJ, Sosnovik DE, Firmin D. In vivo diffusion tensor MRI of the human heart: Reproducibility of breath-hold and navigator-based approaches. Magn Reson Med 2012 Sep 21. doi: 10.1002/mrm.24488. [Epub ahead of print].

2 McGill LA, Ismail TF, Nielles-Vallespin S, Ferreira P, Scott AD, Roughton M, Kilner PJ, Ho SY, McCarthy KP, Gatehouse PD, de Silva R, Speier P, Feiweier T, Mekkaoui C, Sosnovik DE, Prasad SK, Firmin DN, Pennell DJ. Reproducibility of in-vivo diffusion tensor cardiovascular magnetic resonance in hypertrophic cardiomyopathy. J Cardiovasc Magn Reson 2012; 14: 86.

Content

Compressed Sensing: A Great Opportunity to Shift the Paradigm of Cardiac MRI to Real-Time

Michael O. Zenge, Ph.D.

Siemens AG, Healthcare Sector, Erlangen, Germany

In the clinical practice of magnetic resonance imaging (MRI) today, a comprehensive cardiac examination is considered one of the most challenging tasks. In this context, the Cardiac Dot Engine offers a useful tool to achieve reproducible image quality in a standardized and time-efficient way which can be tailored to the specific requirements of an individual institution. However, this approach cannot completely overcome the limitations of ECG-gated acquisitions and the necessity to acquire multiple images in breath-hold. Thus, cardiac MRI is particularly well suited to benefit from a group of novel image reconstruction methods known as compressed sensing [1] that promise to significantly speed up data

1

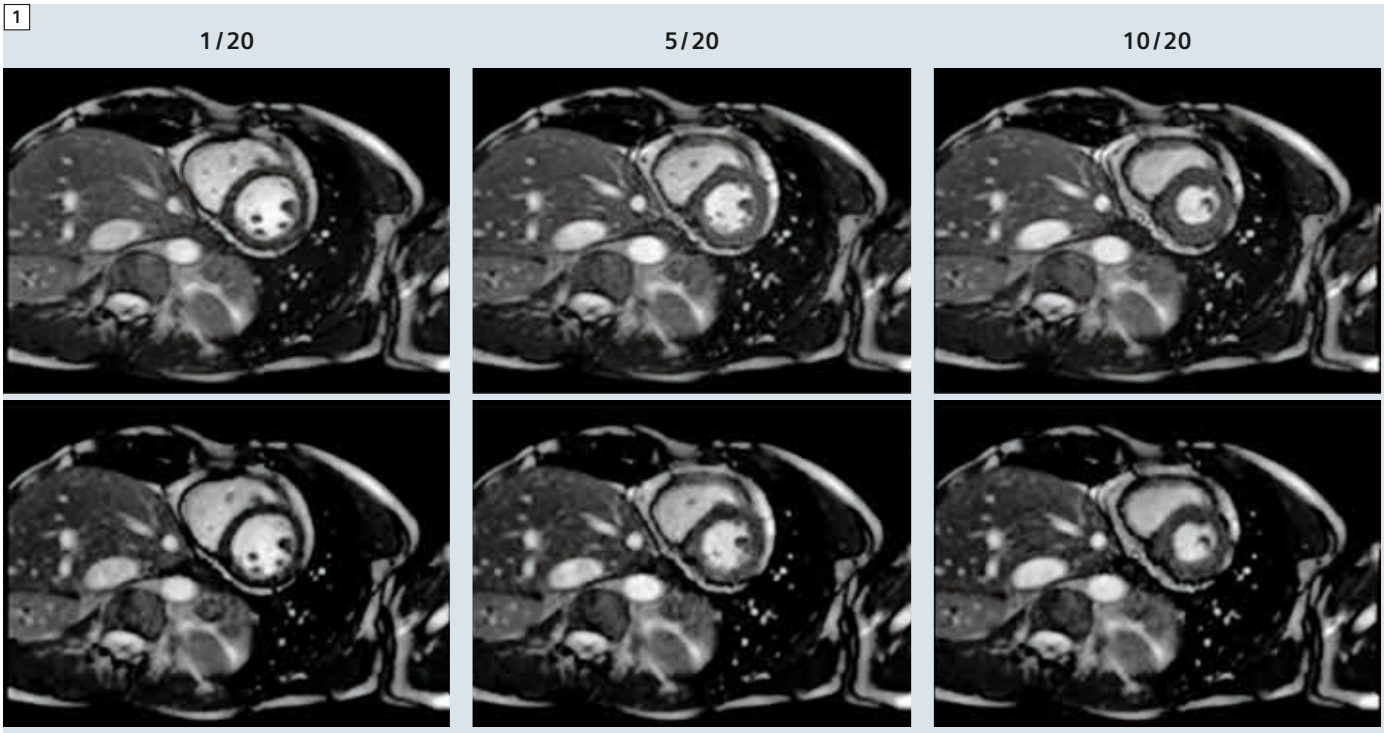

1 Selected time frames of a cardiac CINE MRI, short axis view, temporal resolution 41.3 ms. Comparison of TPAT 2 segmented vs. real-time compressed sensing with net acceleration 7.

acquisition and that could completely change the paradigm of current cardiac imaging.

Compressed sensing methods were introduced to MR imaging [2] just a few years ago and have since been successfully combined with parallel imaging [3]. Such methods try to utilize the full potential of image compression during acquisition of raw input data. Thus, in case of sparse, incoherent sampling, a non-linear iterative optimization avoids sub-sampling artifacts during the process of image reconstruction. Resulting images represent the best solution consistent with the input data, but have a sparse representation in a specific transform domain, e.g. the wavelet domain. In the most favorable case, residual artifacts are not visibly perceptible or are diagnostically irrelevant. One major benefit of compressed sensing compared, for example, to k-t SENSE [4], is that training data is explicitly not required because prior knowledge is formulated very generically.

Very close attention is being paid within the scientific community to compressed sensing and initial experience is promising. To provide broad access for clinical evaluation, the featured solution of compressed sensing [5] has been fully integrated into the Siemens data acquisition and image reconstruction environment. This has enabled real-time CINE MRI with a spatial and temporal resolution that compares to segmented acquisitions (Fig. 1), and first clinical studies have been initiated. In the field of cardiac MRI in particular, a generalization of the current solution, for example, to flow imaging or perfusion, is very likely to be achieved in the near future. This might shift the paradigm to real-time acquisitions in all cases and, in the long run, render cardiac MRI much easier. In this scenario, acquisitions in breath-hold as well as ECG gating will no longer be required. This will not only increase patient comfort and speed up patient preparation but will also add robustness to the entire procedure of cardiac MRI in the future.

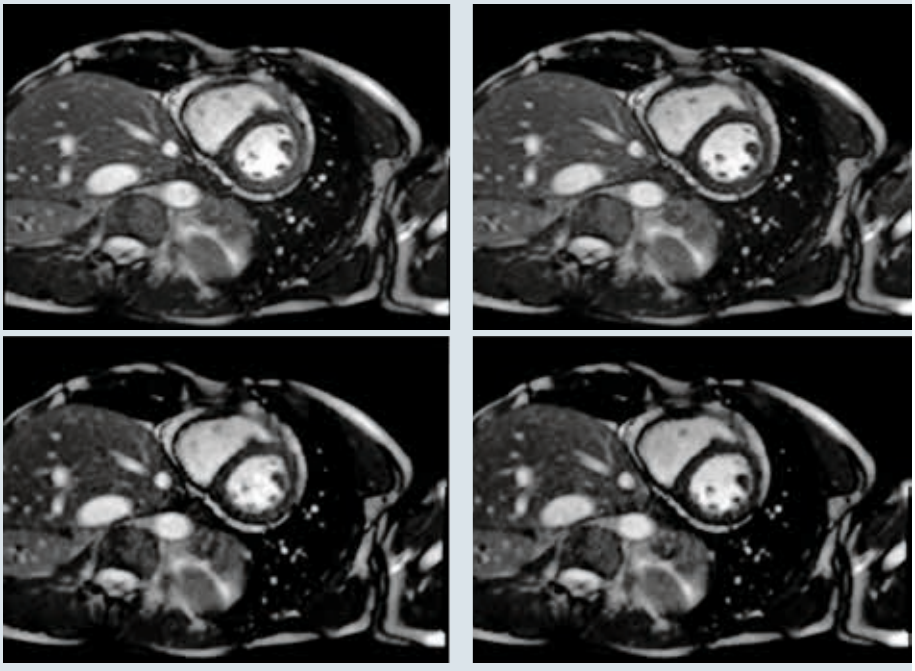

Contact
Michael Zenge, Ph.D.
Siemens AG
Healthcare Sector
IM MR PI CARD
Postbox 32 60
91050 Erlangen
Germany
michael.zenge@siemens.com

References
1 Candes, E.J.; Wakin, M.B.; An Introduction To Compressive Sampling; IEEE Signal Proc Mag., 25:21-30 (2008).
2 Lustig, M.; Donoho, D.; Pauly, J.M.; Sparse MRI: The Application of Compressed Sensing for Rapid MR Imaging; Magn Reson Med. 58:1182-1195 (2007).
3 Liang D.; Liu B.; Wang J.; Ying L.; Accelerating SENSE using compressed sensing; Magn. Reson. Med. 62:1574-84 (2009).
4 Tsao J., Boesiger, P., Pruessmann, K.P.; k-t BLAST and k-t SENSE: Dynamic MRI With High Frame Rate Exploiting Spatiotemporal Correlation; Magn Reson Med. 50:1031-1042 (2003).
5 Liu J. et al.; Dynamic cardiac MRI reconstruction with weighted redundant Haar wavelets; Proc. ISMRM 2012, #178.

Real-Time Low-Latency Cardiac Imaging Using Through-Time Radial GRAPPA

Haris Saybasili, Ph.D.[1]; Bruce Spottiswoode, Ph.D.[2]; Jeremy Collins, M.D.[3]; Sven Zuehlsdorff, Ph.D.[2]; Mark Griswold, Ph.D.[1,4]; Nicole Seiberlich, Ph.D.[1]

[1]*Department of Biomedical Engineering, Case Western Reserve University, Cleveland, OH, USA*
[2]*Siemens Healthcare, Chicago, IL, USA*
[3]*Department of Radiology, Northwestern University, Chicago, IL, USA*
[4]*Department of Radiology, University Hospitals of Cleveland and Case Western Reserve University, Cleveland, OH, USA*

Introduction

Segmented cine imaging using balanced steady state free precession (bSSFP) has been accepted as a gold standard for assessing myocardial function. However, in order to assess the entire volume of the heart, this method requires multiple breath-holds to minimize respiratory motion, which may not be possible for very ill or uncooperative patients. Additionally, due to the signal averaging in segmented cine imaging, it is difficult to achieve reliable imaging in patients with arrhythmias, and even to assess diastolic dysfunction in patients with regular sinus rhythm.

Single-shot, ungated, free-breathing real-time Cartesian MRI is currently unable to match both the temporal and spatial resolution requirements of cardiac MRI. The SCMR recommends at least 50 ms temporal resolution for a clinically acceptable cardiac function assessment [1]. However, this temporal resolution is only possible by sacrificing spatial resolution, or overall image quality, with existing Cartesian real-time MRI methods. Radial acquisitions are more tolerant to undersampling than Cartesian acquisitions due to the oversampled central *k*-space and incoherent aliasing artifacts. However, the degree of undersampling required to match the temporal resolution recommended by the SCMR for cardiac studies may still lead to significant aliasing artifacts. For this reason, several parallel imaging reconstruction strategies for accelerated radial imaging have been proposed to increase the temporal resolution without sacrificing image quality, including *k*-space domain radial GRAPPA [2, 3] and image domain iterative Conjugate Gradient SENSE [4] methods. Both methods yield good image quality with very high acceleration rates.

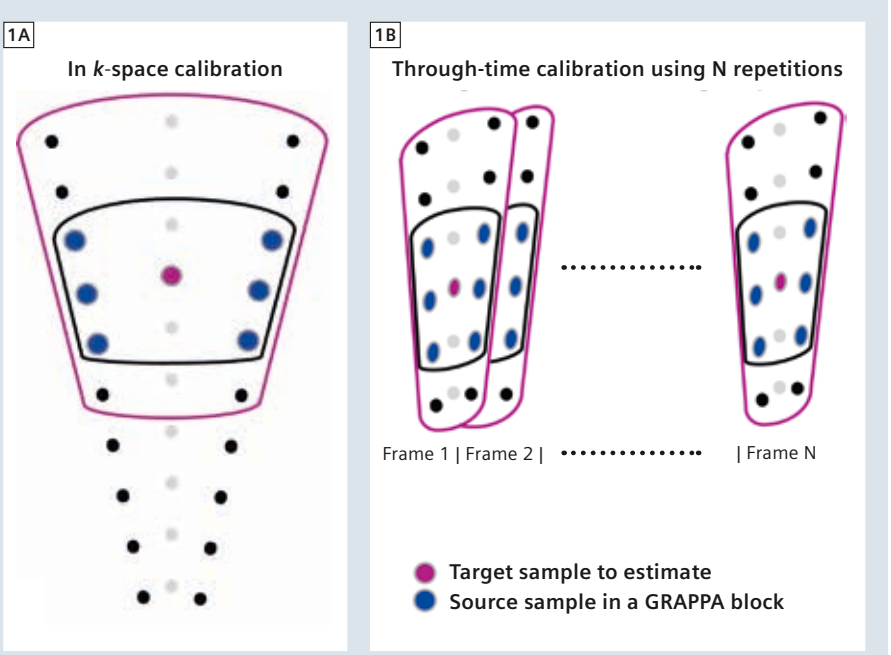

1 Depiction of the hybrid through-time/through-*k*-space radial GRAPPA calibration process. **(1A)** Through-*k*-space calibration with a small segment alone does not yield the necessary number of kernel repetitions to calculate the GRAPPA weights **(1B)** Through-time calibration, using multiple calibration frames, allows the weights to be estimated for the local geometry. The GRAPPA kernel is assumed to be uniform, and the same segment is observed through-time to obtain enough data to solve the inverse problem.

This work describes a through-time radial GRAPPA implementation capable of reconstructing images with both high temporal and spatial resolution which can be used for real-time cardiac acquisitions. Radial GRAPPA is similar to the Cartesian GRAPPA, in that missing *k*-space points are synthesized by convolving acquired points with a GRAPPA kernel. However, due to the non-uniform radial undersampling pattern in *k*-space, a single kernel cannot be used to estimate all the missing samples in the radial case. In the original formulation described by Griswold et al. [2], *k*-space is divided into small segments and reconstructed using one GRAPPA kernel per segment, where each segment was treated as a separate Cartesian GRAPPA problem. When working with the high acceleration factors needed for real-time cardiac imaging, this segmentation approach leads to errors in the GRAPPA weights as the segments no longer have the requisite quasi-Cartesian geometry. In order to generate more accurate GRAPPA weights for non-Cartesian trajectories, the through-time non-Cartesian GRAPPA can be employed [3]. In the through-time approach, individual and geometry-specific kernels are calculated for each missing sample for higher accuracy. In order to collect enough repetitions of the kernel to calculate the GRAPPA weights for the local geometry, multiple fully sampled calibration frames each exhibiting the same local geometry are acquired. For cardiac imaging, these calibration frames can be acquired as a separate free-breathing reference scan. This hybrid through-time/through-*k*-space calibration scheme is depicted in Figure 1. Using a small segment (e.g. 4 points in the readout direction and 1 point in the projection direction, or 4 × 1) combined with a long calibration scan (~30 seconds) provides the highest image quality. However, with only a nominal loss in image quality, it is possible to decrease the calibration scan time by increasing the segment size. Figure 2 shows four images reconstructed from a single undersampled dataset using different calibration configurations. Even though longer calibrations provide bet-

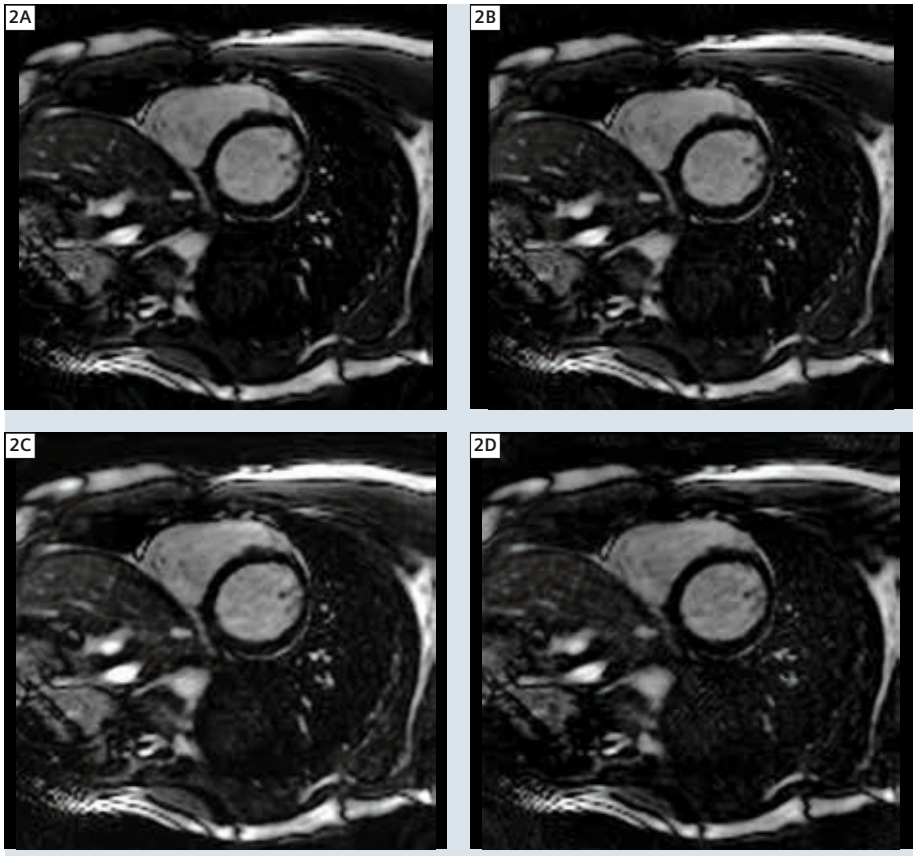

2 Radial GRAPPA reconstruction showing the effect of using a larger segment size to reduce the amount of calibration data required. A long calibration scan provides superior image quality, but adequate image quality can be obtained in a reasonable calibration time using a larger segment. **(2A)** Segment size 4 × 1; calibration frames 80; calibration time 30.4 seconds. **(2B)** Segment size 8 × 4; calibration frames 20; calibration time 7.6 seconds. **(2C)** Segment size 16 × 4; calibration frames 10; calibration time 3.8 seconds. **(2D)** Segment size 24 × 8; calibration frames 2; calibration time 0.8 seconds.

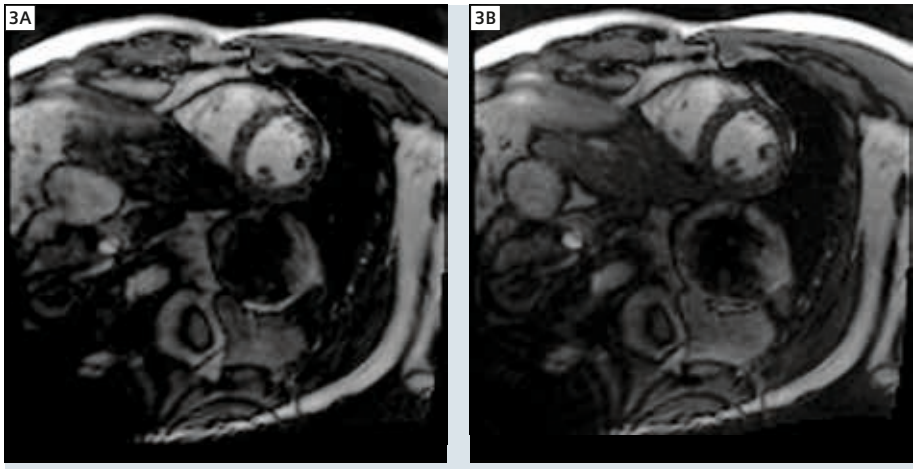

3 Example radial GRAPPA images with varying temporal/spatial resolutions. **(3A)** Short axis view with FOV 300 mm, image matrix 128 × 128, temporal resolution 48 ms, calibration matrix size 128 × 256, accelerated imaging matrix size 16 × 256, radial GRAPPA acceleration rate 8. **(3B)** Short axis view with FOV 300 mm, image matrix 128 × 128, temporal resolution 24 ms, calibration matrix size 128 × 256, accelerated imaging matrix size 8 × 256, radial GRAPPA acceleration rate 16.

ter quality, acceptable images can be obtained using considerably shorter calibration times (~3 seconds). Because image quality can be greatly improved by using additional through-time information, this calibration scheme was implemented for real-time acquisition and reconstruction on the scanner.
Using Tim4G receiver coils, acceleration factors of 16 are achievable, resulting in a 24 ms temporal resolution with a clinically acceptable spatial resolution. Both calibration and reconstruction steps are based on a previous implementation described in Saybasili et al. [5]. The online reconstruction is multi-threaded and GPU-capable, with reconstruction times of less than 100 ms per frame. The calibration process is also multi-threaded. Figure 3 shows example short axis cardiac images acquired with radial GRAPPA acceleration rates of 8 and 16 from a normal volunteer scanned during free breathing on a 3T MAGNETOM Skyra. For assessing functional parameters such as ejection fraction, a user may choose to use lower acceleration rates and benefit from the improved image quality, whereas a higher acceleration rate with lower image quality may be preferable to appreciate detailed myocardial kinetics.
Radial GRAPPA is able to match the spatial resolution of the standard segmented bSSFP cine while providing a higher temporal resolution. Figure 4 compares short-axis cardiac images with the same spatial resolution reconstructed using radial GRAPPA, segmented cine, and Cartesian real-time sequences. While the temporal resolution of segmented cine images was 40 ms, radial GRAPPA provided 25 ms temporal resolution for the same spatial resolution. Cartesian real-time cine images could match neither the temporal or spatial resolution of the segmented cine acquisition. The radial GRAPPA images show considerable improvement compared to the standard Cartesian real-time images, both in spatial and temporal resolution. The segmented cine images are superior in image quality due to averaging, but as a result also lack the temporal fidelity during late diastole, and rely on a consistent breath-hold position.

Clinical case: Left ventricular aneurysm

The patient is a 59-year-old male marathon runner with a past medical history of hyperlipidemia and ST-segment elevation myocardial infarction 5 months ago with symptoms starting while out for a run. The culprit lesion was in the left anterior descending coronary and the patient underwent urgent angiography with bare metal stent placement with an excellent angiographic result. Since then, the patient has resumed running and is asymptomatic, although a recent echocardiogram demonstrated moderate systolic dysfunction with an ejection fraction of 30%. The patient underwent cardiac MR imaging for assessment of ischemic cardiomyopathy. Due to the patient's intermittent arrhythmia, real-time cine imaging was employed. The chamber is enlarged, with wall motion abnormalties in the left anterior descending coronary artery territory, which is predominantly non-viable. There is an apical aneurysm without thrombus, best appreciated on high temporal resolution cine imaging (Fig. 5).

Clinical case: Diastolic dysfunction

The patient is a 64-year-old asymptomatic male with history of hypertension for which he takes two antihypertensive medications. At a routine echocardiography, he was diagnosed with grade I diastolic dysfunction as well as an aortic aneurysm. The patient was referred for cardiac MRI. Real-time cine imaging was performed due to difficulties with breathholding. Impaired myocardial relaxation (grade I diastolic dysfunction) is evident by slowed myocardial relax-

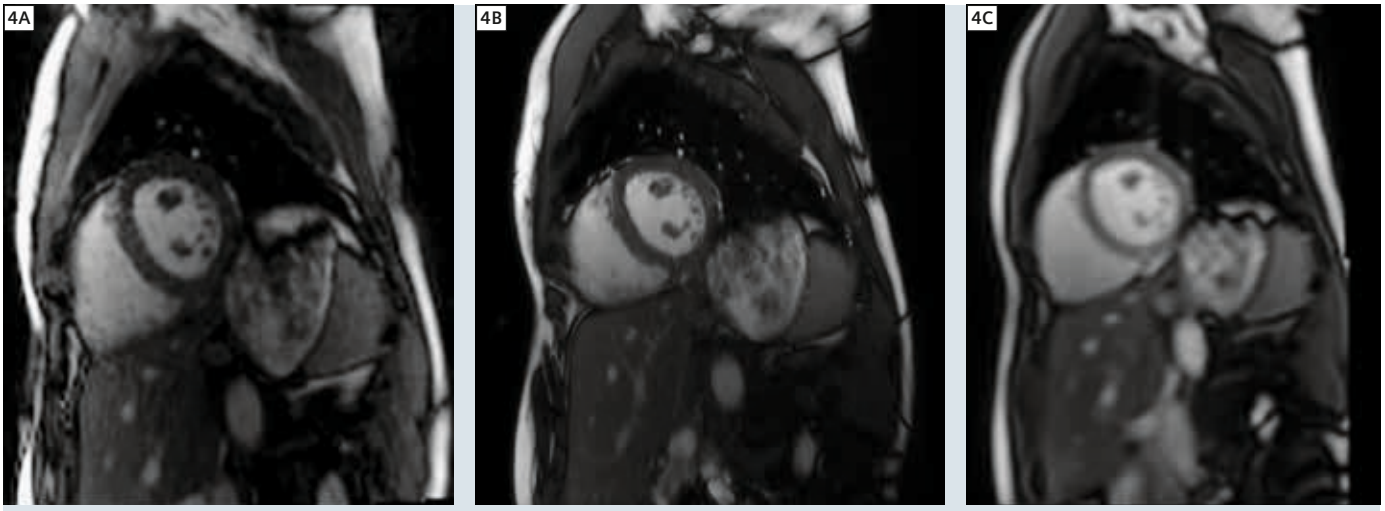

4 Mid ventricular short axis views. **(4A)** Radial GRAPPA, temporal resolution 25 ms, spatial resolution $2 \times 2 \times 8\,mm^3$. **(4B)** Standard product segmented bSSFP cine, temporal resolution 40 ms, spatial resolution $2 \times 2 \times 8\,mm^3$. **(4C)** Cartesian real-time with E-PAT factor 3, temporal resolution 50 ms, spatial resolution $2.8 \times 2.8 \times 8\,mm^3$.

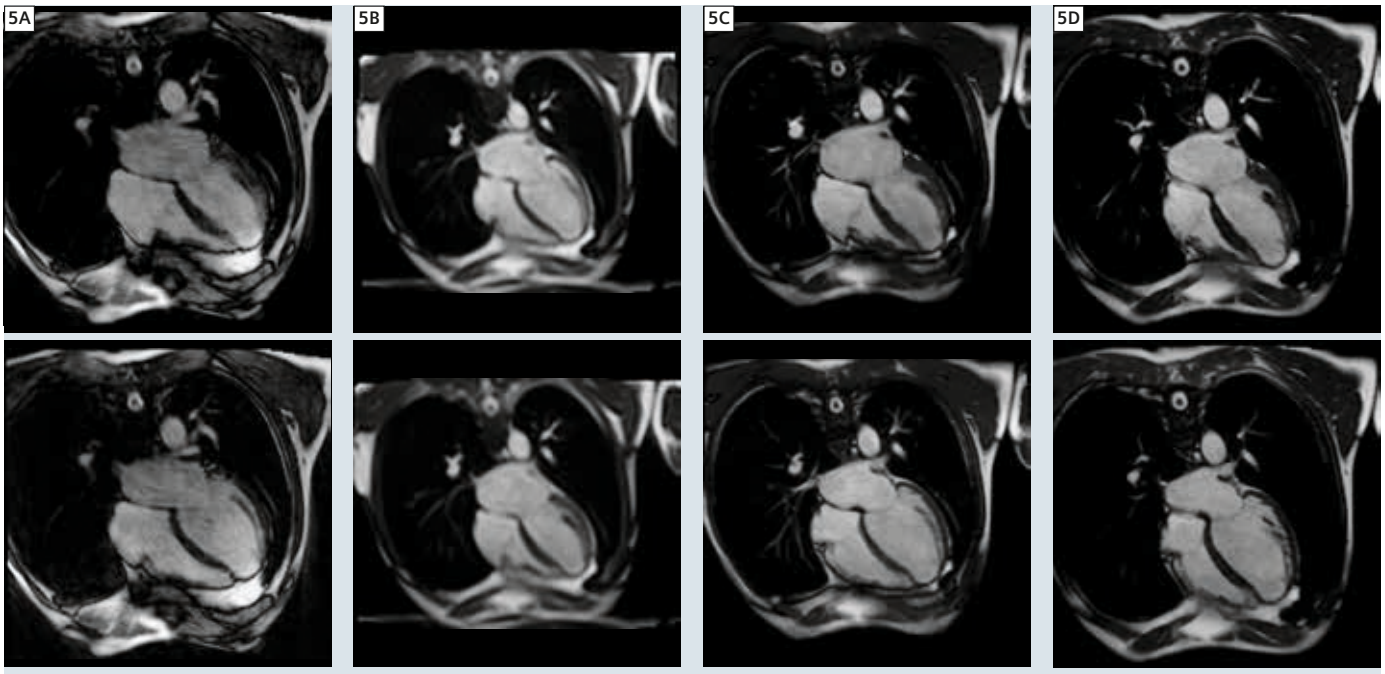

5 **(5A)** Radial GRAPPA bSSFP cine with temporal resolution 25 ms, spatial resolution 1.7 × 1.7 × 8 mm³, radial GRAPPA acceleration rate 16. **(5B)** Cartesian real-time bSSFP cine with E-PAT factor 3, temporal resolution 50 ms, spatial resolution 3 × 3 × 8 mm³. **(5C)** Standard segmented bSSFP cine with temporal resolution 45 ms and spatial resolution 1.7 × 1.7 × 6 mm³. **(5D)** High temporal resolution segmented bSSFP cine acquired in a 22 second breathhold, with temporal resolution 23 ms, and spatial resolution 1.7 × 1.7 × 6 mm³. The top row is end diastole and the bottom row is end systole. The bulging apical aneurism is best appreciated in the high temporal resolution cine images **(5A)** and **(5D)**. The inhomogenity in (5A) is because the intensity normalization was off for the radial GRAPPA sequence and on for all other sequences.

ation on horizontal long axis cine sequences, better appreciated on the highly accelerated real-time radial GRAPPA acquisition.

Please scan the QR-Code® or visit us at **www.siemens.com/diastolic-dysfunction** to see the movies.

Conclusion

Through-time radial GRAPPA is a robust parallel MRI method capable of producing images with high spatial and temporal resolution during un-gated free-breathing real-time acquisitions. Our experiments indicate that through-time radial GRAPPA is capable of matching the spatial resolutions of segmented bSFFP cine acquisitions, while offering higher temporal resolutions, without requiring ECG gating or breath-holding. Additionally, this method outperformed Cartesian real-time acquisitions in term of both spatial and temporal resolutions. The highly optimized multi-threaded CPU implementation (and GPU implementation on supported systems) provides radial GRAPPA estimation performances of 55 – 210 ms per frame (12 – 56 ms on the GPU) for 20 – 30 coil data sets.

This work demonstrates the quality of images that are achievable using high acceleration rates with Tim 4G coils and the acquisition of separate and fully sampled reference data. The technique has the potential to directly improve patient comfort, workflow, and diagnostic potential during a cardiac exam, and deserves consideration for inclusion in current cardiac exam strategies. In addition to imaging sick or uncooperative patients, and patients with arrhythmias, the technique shows promise for assessing diastolic function, perfusion, and real time flow.

Contact
Nicole Seiberlich, Ph.D.
Assistant Professor,
Department of Biomedical Engineering
Case Western Reserve University
Room 309 Wickenden Building
2071 Martin Luther King Jr. Drive
Cleveland, OH, 44106-7207
USA
nes30@case.edu

References
1 Kramer et al. Standardized cardiovascular magnetic resonance imaging (CMR) protocols, society for cardiovascular magnetic resonance: board of trustees task force on standardized protocols. Journal of Cardiovascular Magnetic Resonance 2008, 10:35.
2 Griswold et al. In Proc 12th Annual Meeting of the ISMRM, Kyoto, Japan;2004:737.
3 Seiberlich et al. Improved radial GRAPPA calibration for real-time free-breathing cardiac imaging. Magn Reson Med 2011;65:492-505.
4 Pruessman et al. Advances in sensitivity encoding with arbitrary *k*-space trajectories. Magn Reson Med 2001; 46:638-651.
5 Saybasili et al. Low-Latency Radial GRAPPA Reconstruction using Multi-Core CPUs and General Purpose GPU Programming. Proceedings of the ISMRM 2012, Melbourne, Australia.

Myocardial First-Pass Perfusion Imaging with High Resolution and Extended Coverage Using Multi-Slice CAIPIRINHA

Daniel Stäb, Dipl. Phys.[1,2]; Felix A. Breuer, Ph.D.[3]; Christian O. Ritter, M.D.[1]; Andreas Greiser, Ph.D.[4]; Dietbert Hahn, M.D.[1]; Herbert Köstler, Ph.D.[1,2]

[1]*Institute of Radiology, University of Würzburg, Würzburg, Germany*
[2]*Comprehensive Heart Failure Center (CHFC), Würzburg, Germany*
[3]*Research Center Magnetic Resonance Bavaria (MRB), Würzburg, Germany*
[4]*Siemens Healthcare, Erlangen, Germany*

Background

Contrast-enhanced myocardial first-pass perfusion MR imaging (MRI) is a powerful clinical tool for the detection of coronary artery disease [1–4]. Fast gradient echo sequences are employed to visualize the contrast uptake in the myocardium with a series of saturation prepared images. However, the technique is strictly limited by physiological constraints. Within every RR-interval, only a few slices can be acquired with low spatial resolution, while both high resolution and high coverage are required for distinguishing subendocardial and transmural infarcted areas [5] and facilitating their localization, respectively.
Acceleration techniques like parallel imaging (pMRI) have recently shown their suitability for improving the spatial resolution in myocardial first-pass perfusion MRI [5–7]. Within clinical settings, 3 to 4 slices can be acquired every heartbeat with a spatial resolution of about $2.0 \times 2.0\,mm^2$ in plane [6]. However, for increasing anatomic coverage [8], standard parallel imaging is rather ineffective, as it entails significant reductions of the signal-to-noise ratio (SNR):

a) In order to sample more slices every RR-interval, each single-slice measurement has to be shortened by a certain acceleration factor R, which

1A **Conventional MS-CAIPIRINHA** for coverage extension
Multi-slice excitation and rf phase cycling

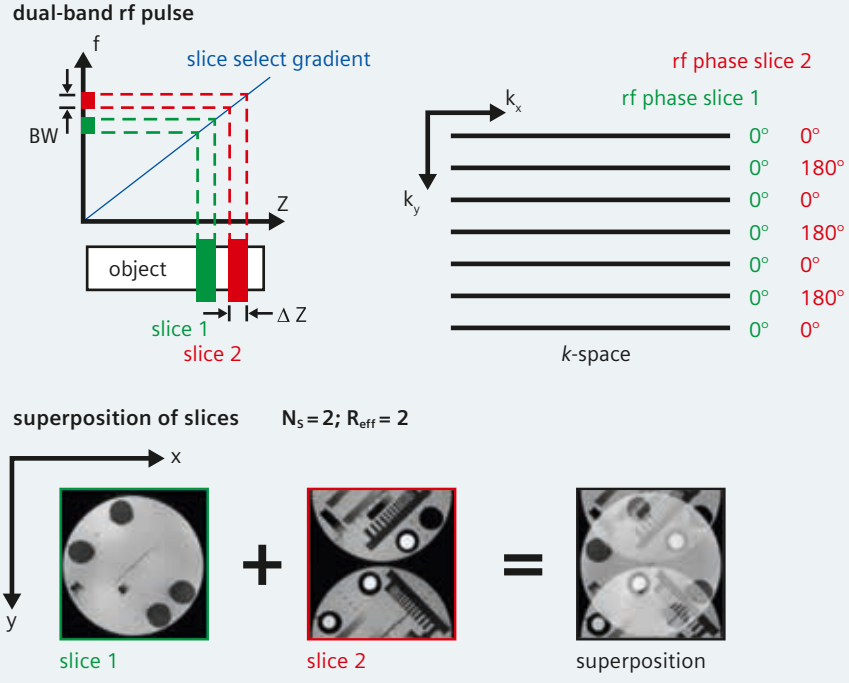

1A MS-CAIPIRINHA with two slices simultaneously excited ($N_S = 2$). A dual-band rf pulse is utilized to excite two slices at the same time (BW = excitation bandwidth). During data acquisition, each slice is provided with an individual rf phase cycle. A slice specific constant rf phase increment is employed (0° in slice 1, 180° in slice 2) between succeeding excitations. Consequently, the two slices appear shifted by ½ FOV with respect to each other. In this way, the overlapping pixels originate not only from different slices, but also from different locations along the phase encoding direction (y), facilitating a robust slice separation using pMRI reconstruction techniques. Using the two-slice excitation, effectively a two-fold acceleration is achieved ($R_{eff} = 2$).

inevitably comes along with an √R-fold SNR reduction.

b) During image reconstruction, the SNR is further reduced by the so-called geometry (g)-factor [9], an inhomogeneous noise-amplification depending on the encoding capabilities of the receiver array.

In addition, unless segmented acquisition techniques are utilized [10], the saturation recovery (SR) magnetization preparation has to be taken into account:

c) The preparation cannot be accelerated itself. Hence, the acceleration factor R has to be higher than the factor by which the coverage is extended. This leads to an increase of the SNR-reduction discussed in (a).

d) Subsequent to the preparation, the signal increases almost linearly with time. Thus, shortening the acquisition by a factor of R is linked to an additional R-fold SNR-loss.

As demonstrated recently [11], most of these limitations can be overcome by employing the **MS-CAIPIRINHA** (**M**ulti-**S**lice **C**ontrolled **A**liasing **I**n **P**arallel **I**maging **R**esults **IN** **H**igher **A**cceleration) concept [12, 13] for simultaneous 2D multi-slice imaging. By simultaneously scanning multiple slices in the time conventionally required for the acquisition of one single slice, this technique enables a significant increase in anatomic coverage. Since image acquisition time is preserved with respect to the single-slice measurement, the technique does not experience any SNR reductions despite the g-factor noise amplification of the required pMRI reconstruction [11, 12]. The MS-CAIPIRINHA concept can also be employed with acceleration factors that are higher than the number of slices excited at the same time. By utilizing this acceleration for increasing spatial resolution, the technique facilitates myocardial first-pass perfusion examinations with extended anatomic coverage and high spatial resolution.

A short overview of the concept is set out below, followed by a presentation of *in-vivo* studies that demonstrate the capabilities of MS-CAIPIRINHA in contrast-enhanced myocardial first-pass perfusion MRI.

1B **MS-CAIPIRINHA with $R_{eff} > N_s$** for improving coverage and resolution
Multi-slice excitation, *k*-space undersampling and rf phase cycling

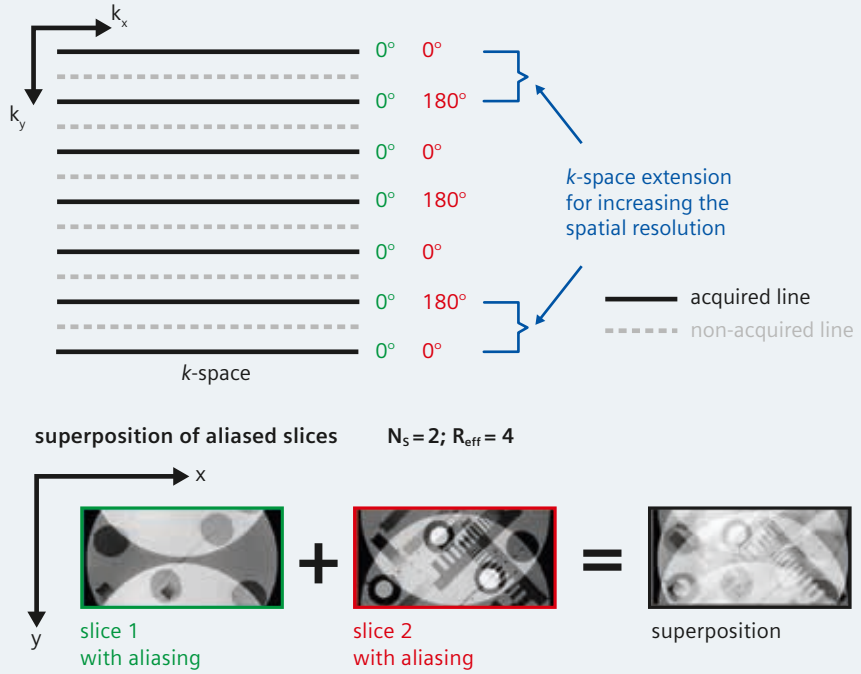

1B MS-CAIPIRINHA with an effective acceleration factor higher than the number of slices excited simultaneously. Again, two slices are excited at the same time employing the same rf phase cycles as in (1A), but *k*-space is undersampled by a factor of two. The slices and their undersampling-induced aliasing artifacts appear shifted with respect to each other by ½ FOV and can be separated using pMRI reconstruction techniques. Effectively, a four-fold acceleration is achieved ($R_{eff} = 4$). The additional acceleration can be employed to extend *k*-space and to improve the spatial resolution.

Improving anatomic coverage and spatial resolution with MS-CAIPIRINHA

MS-CAIPIRINHA

The MS-CAIPIRINHA concept [12, 13] is based on a coinstantaneous excitation of multiple slices, which is accomplished by means of multi-band radiofrequency (rf) pulses (Fig. 1A). Being subject to the identical gradient encoding procedure, the simultaneously excited slices appear superimposed on each other, unless the individual slices are provided with different rf phase cycles. In MS-CAIPIRINHA, the latter is done in a well-defined manner in order to control the aliasing of the simultaneously excited slices. Making use of the Fourier shift theorem, dedicated slice specific rf phase cycles are employed to shift the slices with respect to each other in the field-of-view (FOV) (Fig. 1A). The slice separation is performed using pMRI reconstruction techniques. However, the shift of the slices causes superimposed pixels to originate from not only different slices, but also different locations along the phase encoding direction. Thus, the MS-CAIPIRINHA concept allows the pMRI reconstruction to take advantage of coil sensitivity variations along two dimensions and to perform the slice separation with low g-factor noise amplification [12].

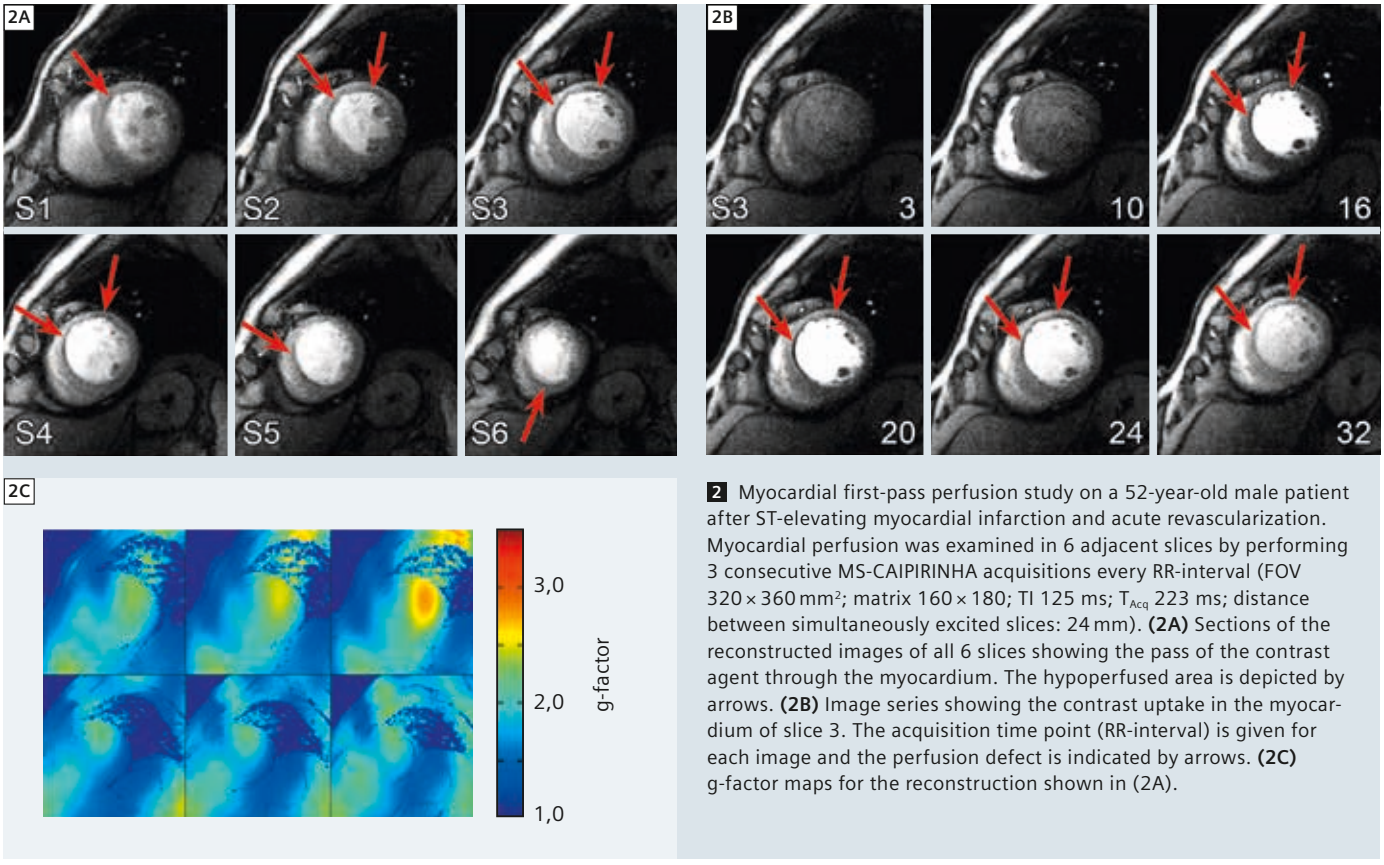

2 Myocardial first-pass perfusion study on a 52-year-old male patient after ST-elevating myocardial infarction and acute revascularization. Myocardial perfusion was examined in 6 adjacent slices by performing 3 consecutive MS-CAIPIRINHA acquisitions every RR-interval (FOV 320 × 360 mm²; matrix 160 × 180; TI 125 ms; T_{Acq} 223 ms; distance between simultaneously excited slices: 24 mm). **(2A)** Sections of the reconstructed images of all 6 slices showing the pass of the contrast agent through the myocardium. The hypoperfused area is depicted by arrows. **(2B)** Image series showing the contrast uptake in the myocardium of slice 3. The acquisition time point (RR-interval) is given for each image and the perfusion defect is indicated by arrows. **(2C)** g-factor maps for the reconstruction shown in (2A).

By conserving image acquisition time with respect to an equivalent single-slice measurement, the technique is not subject to any further SNR penalties. MS-CAIPIRINHA hence allows extending the coverage in 2D multi-slice imaging in a very efficient manner. Applied to myocardial first-pass perfusion imaging, the concept facilitates the acquisition of 6 slices every heartbeat with an image quality that is comparable to that of conventional 3-slice examinations [11].

Additional acceleration

While extending the coverage can be accomplished by simultaneous multi-slice excitation, improving the spatial resolution requires additional *k*-space data to be sampled during image acquisition. Of course, as the FOV and the image acquisition time are to be conserved, this can only be achieved by means of additional acceleration. However, the effective acceleration factor of MS-CAIPIRINHA is not restricted to the number of slices excited simultaneously. By applying simultaneous multi-slice excitation to an imaging protocol with reduced phase FOV, i.e. equidistant *k*-space undersampling, supplementary in-plane acceleration can be incorporated (Fig. 1B). The rf phase modulation forces the two simultaneously excited slices and their in-plane aliasing artifacts to be shifted with respect to each other in the FOV. As before, image reconstruction and slice separation is performed utilizing pMRI methods. Employed like this, the MS-CAIPIRINHA concept facilitates an increase of both, anatomic coverage and spatial resolution with high SNR efficiency. Since image acquisition time does not have to be shortened, SNR is only affected by the voxel size and the noise amplification of the pMRI reconstruction.

Imaging

Perfusion datasets were obtained from several volunteers and patients. The study was approved by the local Ethics Committee and written informed consent was obtained from all subjects. All examinations were performed on a clinical 3T MAGNETOM Trio, a Tim system (Siemens AG, Healthcare Sector, Erlangen, Germany), using a dedicated 32-channel cardiac array coil (Siemens AG, Healthcare Sector, Erlangen, Germany) for signal reception. Myocardial perfusion was assessed using a SR FLASH sequence (FOV 320 × 300-360 mm²; matrix 160 × 150-180; TI 110-125 ms; TR 2.8 ms; TE 1.44 ms; T_{Acq} 191-223 ms; slice thickness 8 mm; flip angle 12°). Two slices were excited at the same time (distance between simultaneously excited slices: 24-32 mm) and shifted by ½ FOV with respect to each other by respectively providing the first and second slice with a 0° and 180° rf phase cycle. In order to realize a spatial resolution of 2.0 × 2.0 mm² within the imaging plane, *k*-space was undersampled by a factor of 2.5, resulting in an overall effective acceleration factor of 5.

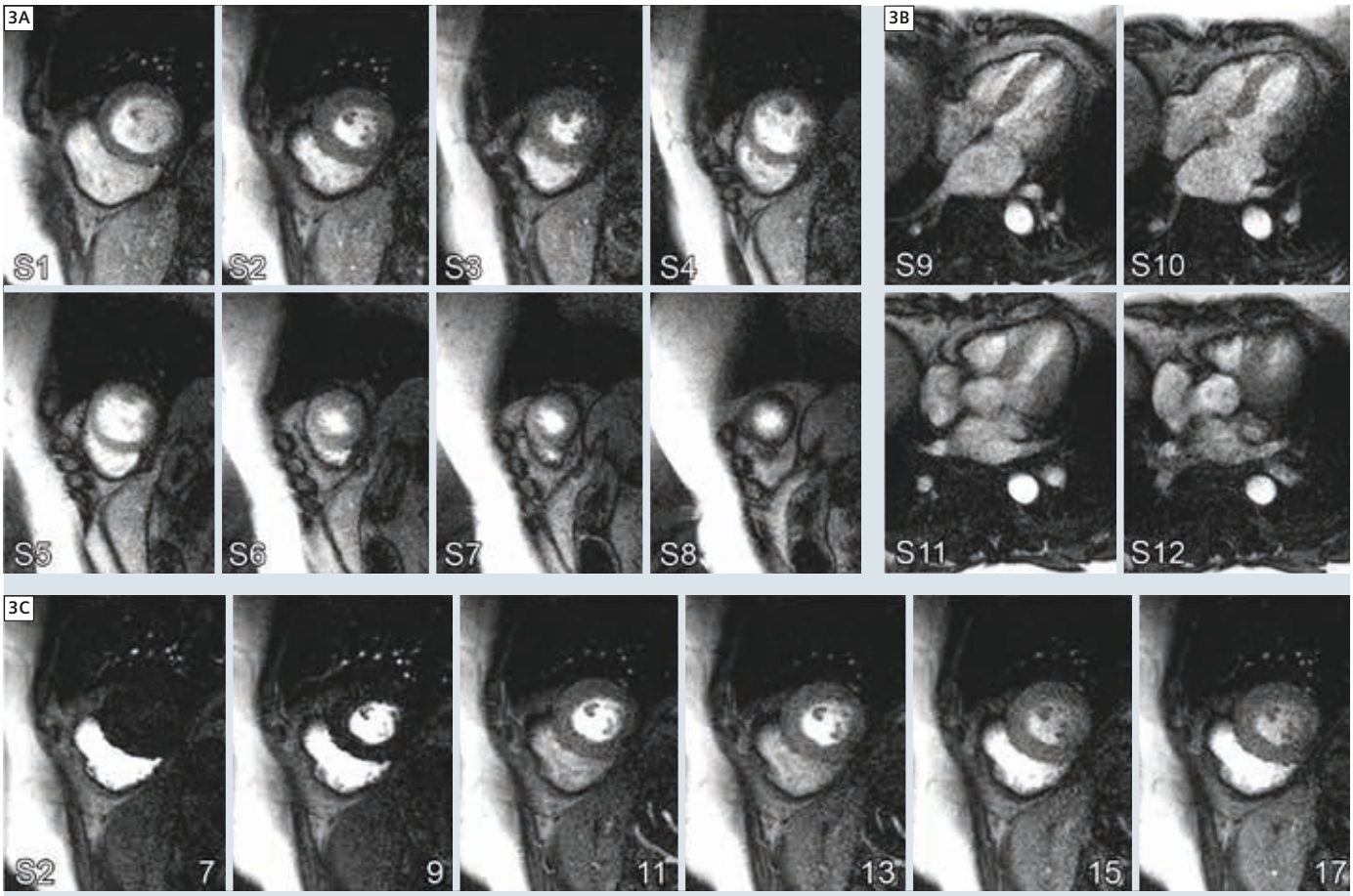

3 Myocardial first-pass perfusion study on a 51-year-old female volunteer with whole heart coverage. 6 consecutive MS-CAIPIRINHA acquisitions were performed every two RR-intervals (FOV 320 × 300 mm²; matrix 160 x 150; TI 110 ms; T_{Acq} 191 ms; distance between simultaneously excited short/long axis slices: 32/16 mm). **(3A)** Sections of the reconstructed short axis images. **(3B)** Sections of the reconstructed long axis images. **(3C)** Series of image sections showing the contrast uptake in the myocardium of slice 2. The acquisition time point (RR-interval) is given for each image. **(3D)** g-factor maps for the reconstructions shown in (3A). **(3E)** g-factor maps for the reconstructions shown in (3B). **(3F)** Measurement scheme. The acquisition was performed with a temporal resolution of 1 measurement every 2 RR-intervals.

All first-pass perfusion measurements were conducted in rest over a total of 40 heartbeats. All subjects were asked to hold their breaths during the acquisition as long as possible. Every RR-interval, 3 to 4 consecutive MS-CAIPIRINHA acquisitions were performed in order to sample the contrast uptake of the myocardium. For contrast enhancement, a contrast agent bolus (4 ml, Gadobutrol, Bayer HealthCare, Berlin, Germany) followed by a 20 ml saline flush was administered at the beginning of each perfusion scan. Image reconstruction was performed using an offline GRAPPA [14] reconstruction. The according weights were determined from a separate full FOV calibration scan. To evaluate the GRAPPA reconstruction, an additional noise scan was obtained and the g-factor noise enhancement was quantified [15]. All calculations were performed on a standalone PC using Matlab (The MathWorks, Natick, MA, USA).

Results

Figure 2 shows the results of a myocardial first-pass perfusion examination with 6-slices on a 52-year-old male patient (91 kg, 185 cm) on the fourth day after STEMI (ST-elevating myocardial infarction) and acute revascularization. Sections of the reconstructed images of all examined slices are depicted, showing the first pass of contrast agent through the myocardium (Fig. 2A). Also displayed is a series of image sections demonstrating contrast uptake in slice 3 (Fig. 2B). The GRAPPA reconstruction separated the simultaneously excited slices without visible artifacts. The g-factor maps (Fig. 2C) indicate generally low noise amplification. Thus, in comparison to the high effective acceleration factor of 5, the images provide excellent image quality. Both contrast and SNR allow for a clear delineation of the subendocardial hypoperfused area within the anterior and septal wall of the myocardium (arrows).

The results of a first-pass perfusion study with whole heart coverage are displayed in Fig. 3. In a 51-year-old female volunteer, first pass perfusion was examined in eight short (Fig. 3A) and four long axis slices (Fig. 3B). In order to accomplish the 12-slice examination and to achieve whole heart coverage, temporal resolution was reduced by a factor of two with respect to the examination displayed in Fig. 2. The contrast uptake of the myocardium was sampled with 1 measurement every two RR-intervals by performing 3 out of 6 consecutive double-slice MS-CAIPIRINHA acquisitions every heartbeat (Fig. 3F). Image reconstruction could be performed without visible artifacts and generally low noise amplification (Figs. 3D and E). Only in a few regions, the g-factor maps show moderate noise enhancement. In the images, the myocardium is homogeneously contrasted and the contrast agent uptake is clearly visible (Fig. 3C).

The findings of a first-pass perfusion study in a 48-year-old male patient (80 kg, 183 cm) on the eighth day after STEMI and acute revascularization are presented in Fig. 4. An overall of 8 slices were acquired with a temporal resolution of 1 measurement every RR-interval by performing 4 consecutive MS-CAIPIRINHA acquisitions after each ECG trigger pulse. Sections of the reconstructed images, showing the first pass of contrast agent through the myocardium in all 8 slices (Fig. 4A) are depicted together with sections demonstrating the process of contrast uptake in slice 5 (Fig. 4B). Despite the breathing motion (Fig. 4D), the GRAPPA reconstruction performed robustly and separated the slices without significant artifacts. The g-factor noise amplification is generally low and moderate within a few areas (Fig. 4C). In the images, the hypoperfused subendocardial region in the anterior wall can be clearly identified (arrows). As can be seen from the enlarged section of slice 5 (Fig. 4F), the technique provides sufficient spatial resolution to distinguish between subendocardial and transmural perfusion defects. These findings correspond well to the results of a subsequently performed Late Enhancement study (Fig. 4E) delineating a transmural infarction zone of the anterior wall (midventricular to apical).

Discussion

Contrast-enhanced myocardial first-pass perfusion MRI with significantly extended anatomic coverage and high spatial resolution can be successfully performed by employing the MS-CAIPIRINHA concept for simultaneous multi-slice imaging. Basically, two different acceleration approaches are combined: the simultaneous excitation of two slices on the one hand and *k*-space undersampling on the other. While the first directly doubles the number of slices acquired, the second provides sufficient acceleration for improving the spatial resolution. The proposed imaging protocols provide an effective acceleration factor of 5, which is sufficient for the acquisition of 6 to 8 slices every RR-interval with a high spatial resolution of $2.0 \times 2.0 \times 8\,mm^3$. Correspondingly, whole heart coverage can be achieved by sampling 12 slices with a temporal resolution of 1 measurement every 2 RR-intervals. Since the slices can be planned with individual thickness and pairwise specific orientation, the concept thereby provides high flexibility. With image acquisition times of 191 ms, it also supports stress examinations in 6 slices up to a peak heart rate of 104 bpm.

Employing a dedicated 32-channel cardiac array coil, the image reconstructions could be performed without significant reconstruction artifacts and only low to moderate g-factor noise amplification. Also in presence of breathing motion, the GRAPPA reconstruction performed robustly. The images provided sufficient SNR and contrast between blood, myocardium and lung tissue to delineate small perfusion defects and to differentiate between subendocardial and transmural hypoperfused areas.

Compared to conventional parallel MRI, the MS-CAIPIRINHA concept benefits from the high SNR efficiency discussed earlier. Simultaneous multi-slice excitation allows increasing the coverage without supplementary *k*-space under-

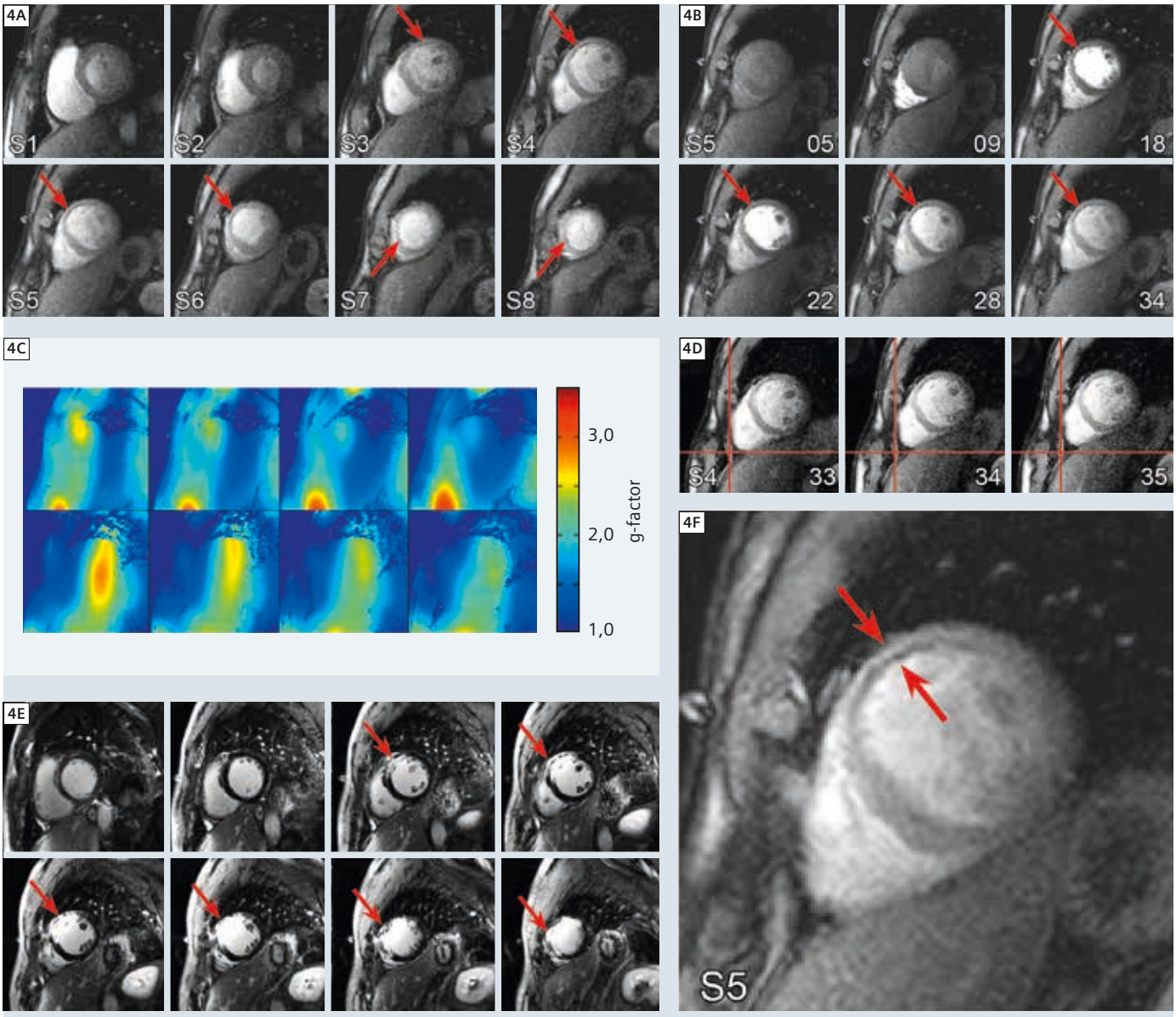

4 Myocardial first-pass perfusion study on a 48-year-old male patient after ST-elevating myocardial infarction and acute revascularization. 8 slices were acquired every RR-interval by performing 4 consecutive MS-CAIPIRINHA acquisitions (FOV 320 × 300 mm²; matrix 160 × 150; TI 110 ms; T_{Acq} 191 ms; flip angle 10°; distance between simultaneously excited slices: 32 mm). **(4A)** Sections of the reconstructed images of all 8 slices showing the first pass of the contrast agent through the myocardium. The hypoperfused area is depicted by arrows. **(4B)** Image series showing the contrast uptake in the myocardium of slice 5. The acquisition time point (RR-interval) is given for each image and the perfusion defect is indicated by arrows. **(4C)** g-factor maps for the reconstruction shown in (4A). **(4D)** Displacement of the heart due to breathing motion, example for slice 4. **(4E)** Late gadolinium enhancement. **(4F)** Enlarged section of slice 5. The technique allows distinguishing between subendocardial and transmural perfusion defects.

sampling. At the same time the g-factor noise amplification is minimized by exploiting coil sensitivity variations in both, slice and phase encoding direction. Thus, despite the doubled anatomic coverage, the image quality obtained is comparable to that of an accelerated measurement with standard coverage and high spatial resolution [5]. An important feature of the MS-CAIPIRINHA concept in myocardial first-pass perfusion MRI is the frame-by-frame reconstruction, which prevents the reconstructed images to be affected by temporal blurring. Moreover, arrhythmia and breathing motion only impact the underlying time frame and not the whole image series, as it is likely for reconstruction techniques incorporating the temporal domain [16–19].

Simultaneous multi-slice excitation is, of course, linked to an increase in the amount of energy that is deployed to the subject under investigation. Thus, limitations have to be expected at higher field strengths or when using sequences with larger flip angles, such as TrueFISP. At 1.5 Tesla, the application of the MS-CAIPIRINHA concept to TrueFISP has been successfully demonstrated utilizing advanced rf phase cycling [11].
In all *in-vivo* examinations, the distance between the two slices excited simultaneously was maximized in order to make use of the highest possible coil sensitivity variations in slice direction and to minimize the g-factor penalty. Thus, the spatial distance between consecutively acquired cardiac phases is large which might be a possible drawback for correlating hypoperfused regions of the myocardium. While the latter was feasible for all *in-vivo* studies, slice distance naturally can be reduced at the expense of slightly more noise enhancement.

Conclusion

Utilizing the MS-CAIPIRINHA concept for simultaneous multi-slice imaging, contrast-enhanced myocardial first-pass perfusion MRI can be performed with an anatomic coverage of 6 to 8 slices every heart beat and a high spatial resolution of $2.0 \times 2.0 \times 8\,mm^3$. Based on the simultaneous excitation of multiple slices, the concept provides significantly higher SNR than conventional in-plane acceleration techniques with identical acceleration factor and facilitates an accurate image reconstruction with only low to moderate g-factor noise amplification. Taking into account the high flexibility, simple applicability and short reconstruction times in addition to the high robustness in presence of breathing motion or arrhythmia, the concept can be considered a promising candidate for clinical perfusion studies.

Acknowledgements

The authors would like to thank the Deutsche Forschungsgemeinschaft (DFG) *and* the Federal Ministry of Education and Research (BMBF), Germany *for grant support.*

Contact
Daniel Stäb
Institute of Radiology
University of Würzburg
Oberdürrbacher Str. 6
97080 Würzburg
Germany
staeb@roentgen.uni-wuerzburg.de

References

1 Atkinson DJ, Burnstein D, Edelman RR. First-pass cardiac perfusion: evaluation with ultrafast MR imaging. Radiology 1990; 174:757–762.
2 Wilke N, Jerosch-Herold M, Wang Y, Yimei H, Christensen BV, Stillman E, Ugurbil K, McDonald K, Wilson RF. Myocardial Perfusion Reserve: Assessment with Multisection, Quantitative, First-Pass MR Imaging. Radiology 1997; 204:373–384.
3 Rieber J, Huber A, Erhard I, Mueller S, Schweyer M, Koenig A, Schiele TM, Theisen K, Siebert U, Schoenberg SO, Reiser M, Klauss V. Cardiac magnetic resonance perfusion imaging for the functional assessment of coronary artery disease: a comparison with coronary angiography and fractional flow reserve. Eur Heart J 2006; 27:1465–1471.
4 Schwitter J, Nanz D, Kneifel S, Bertschinger K, Büchi M, Knüsel PR, Marincek B, Lüscher TF, Schulthess GK. Assessment of Myocardial Perfusion in Coronary Artery Disease by Magnetic Resonance. Circulation 2001; 103:2230–2235.
5 Ritter CO, del Savio K, Brackertz A, Beer M, Hahn D, Köstler H. High-resolution MRI for the quantitative evaluation of subendocardial and subepicardial perfusion under pharmacological stress and at rest. RoFo 2007; 179:945–952.
6 Strach K, Meyer C, Thomas D, Naehle CP, Schmitz C, Litt H, Bernstein A, Cheng B, Schild H, Sommer T. High-resolution myocardial perfusion imaging at 3 T: comparison to 1.5 T in healthy volunteers. Eur Radiol 2007; 17:1829–1835.
7 Jung B, Honal M, Hennig J, Markl M. k-t-Space accelerated myocardial perfusion. J Magn Reson Imag 2008; 28:1080–1085.
8 Köstler H, Sandstede JJW, Lipke C, Landschütz W, Beer M, Hahn D. Auto-SENSE perfusion imaging of the whole human heart. J Magn Reson Imag 2003; 18:702–708.
9 Pruessmann KP, Weiger M, Scheidegger MB, Boesiger P. SENSE: sensitivity encoding for fast MRI. Magn Reson Med 1999; 42:952–962.
10 Kellman P, Derbyshire JA, Agyeman KO, McVeigh ER, Arai AE. Extended coverage first-pass perfusion imaging using slice-interleaved TSENSE. Magn Reson Med 2004; 51:200–204.
11 Stäb D, Ritter CO, Breuer FA, Weng AM, Hahn D, Köstler H. CAIPIRINHA accelerated SSFP imaging. Magn Reson Med 2011; 65:157–164.
12 Breuer FA, Blaimer M, Heidemann RM, Mueller MF, Griswold MA, Jakob PM. Controlled aliasing in parallel imaging results in higher acceleration (CAIPIRINHA) for multi-slice imaging. Magn Reson Med 2005; 53:684–691.
13 Breuer F, Blaimer M, Griswold M, Jakob P. Controlled Aliasing in Parallel Imaging Results in Higher Acceleration (CAIPIRINHA). Magnetom Flash 2012; 49:135–142.
14 Griswold MA, Jakob PM, Heidemann RM, Nittka M, Jellus V, Wang J, Kiefer B, Haase A. Generalized autocalibrating partially parallel acquisitions (GRAPPA). Magn Reson Med 2002; 47:1202–1210.
15 Breuer FA, Kannengiesser SAR, Blaimer M, Seiberlich N, Jakob PM, Griswold MA. General formulation for quantitative G-factor calculation in GRAPPA reconstructions. Magn Reson Med 2009; 62:739–746.
16 Adluru G, Awate SP, Tasdizen T, Whitaker RT, Dibella EVR. Temporally constrained reconstruction of dynamic cardiac perfusion MRI. Magn Reson Med 2007; 57: 1027–1036.
17 Otazo R, Kim D, Axel L, Sodickson DK. Combination of compressed sensing and parallel imaging for highly accelerated first-pass cardiac perfusion MRI. Magn Reson Med 2010; 64:767–776.
18 Ge L, Kino A, Griswold M, Mistretta C, Carr JC, Li D. Myocardial perfusion MRI with sliding-window conjugate-gradient HYPR. Magn Reson Med 2009; 62:835–839.
19 Plein S, Kozerke S, Suerder D, Luescher TF, Greenwood JP, Boesiger P, Schwitter J. High spatial resolution myocardial perfusion cardiac magnetic resonance for the detection of coronary artery disease. Eur Heart J 2008; 29:2148–2155.

Evaluating cardiac flow data is now automated thanks to *syngo*.via.[1]

Patients with compromised cardiac function require a more comprehensive evaluation to determine areas of significant pathology. A key step in this process includes cardiac flow quantification, which typically involves many labor-intensive steps. *syngo*®.via eliminates the need for most cumbersome tasks, providing a more streamlined workflow.

- Time saving automation provides results quicker.
- *syngo*.via compensates for up to 200 % inaccuracy in velocity encoding values, helping to avoid repeat scans[2]
- Integrated reporting enables flow results to be accessible everywhere.

[1] *syngo*.via can be used as a standalone device or together with a variety of *syngo*.via-based software options, which are medical devices in their own rights.

[2] May not work in all situations. Please ensure proper VENC values by running a VENC-scout, and then setting the VENC for the diagnostic scan based on the outcome of the VENC-scout. In situations where the VENC was still set too low, despite the results of the scout, the anti-aliasing tool (part of *syngo*.MR Cardiac Flow) can be used to correct for inaccuracy in the VENC values and alleviate the resulting aliasing artifacts. Do not misuse this tool and intentionally set VENC values at a lower than optimal rate as the VENC anti-aliasing function will not work in 100% of the cases.

Acceleration of Velocity Encoded Phase Contrast MR. New Techniques and Applications

Jennifer A Steeden; Vivek Muthurangu

Vascular Imaging and Physics Group, UCL Centre for Cardiovascular Imaging, London, UK

1

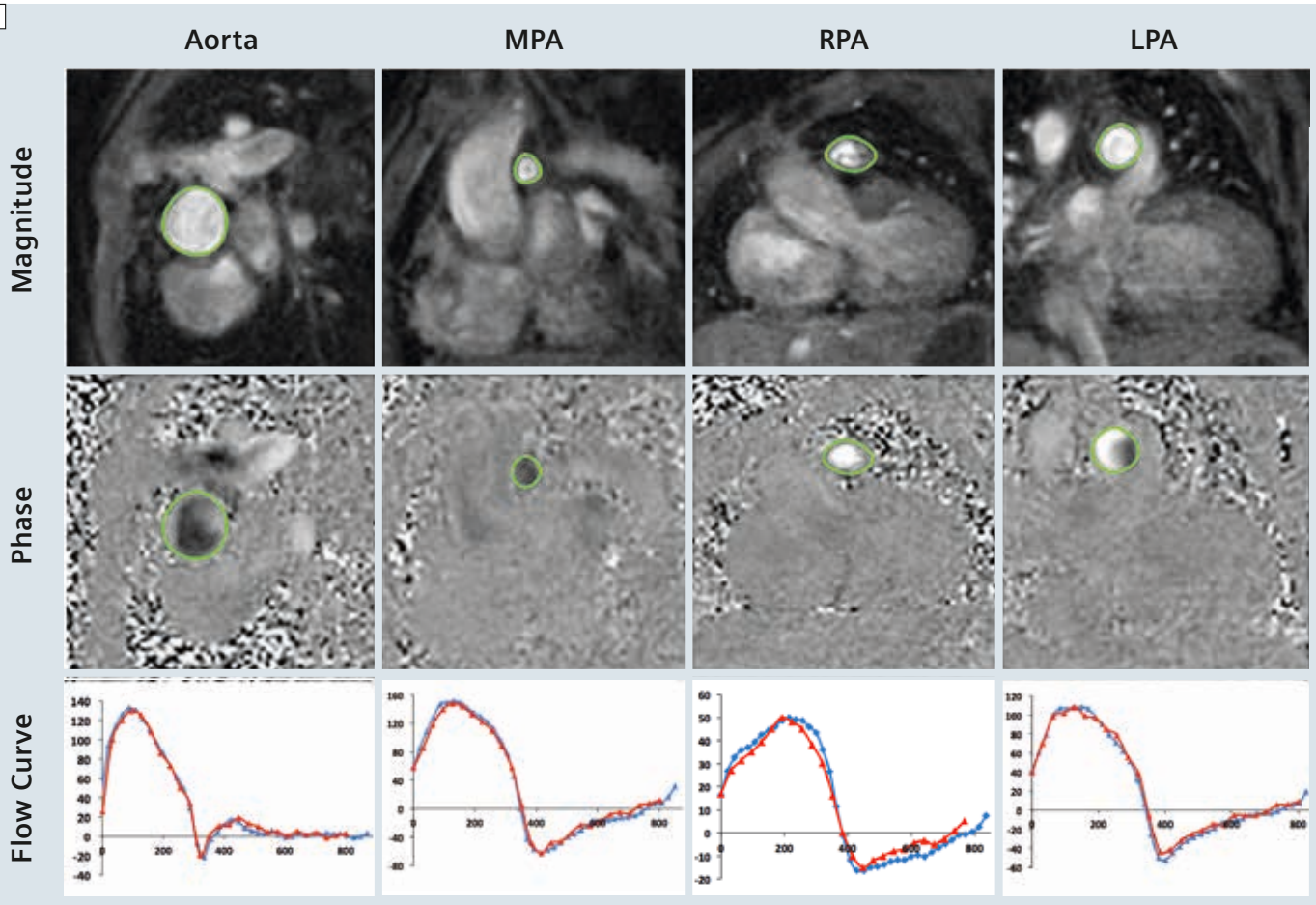

1 Rapid Cardiac-Gated PCMR achieved using undersampled spiral trajectories, in a child, age 2 years. Flow curves show good agreement with a conventional Cartesian acquisition throughout the entire cardiac cycle (blue: retrospectively-gated Cartesian PCMR acquisition, red: prospectively-gated undersampled spiral acquisition).

Introduction

The cardiovascular system is characterized by motion, whether that be of the blood, the myocardium or the valves. For this reason, cardiovascular disease is often associated with abnormalities in flow and movement. Thus, assessment of motion is a vital part of the cardiovascular work-up. One of the most important methods of assessing motion is to measure the velocity of a moving structure and this is an area in which cardiovascular magnetic resonance (CMR) has an important role to play. In fact, CMR has become the gold standard method of assessing volume blood flow in conditions such as congenital heart disease. However, velocity encoded CMR techniques are slow and this has limited their uptake in some clinical situations. In this review we will address novel acceleration techniques that are opening up new areas for CMR velocity quantification.

Basic CMR velocity encoding

The CMR technique that is most commonly used to measure velocity is phase contrast MR (PCMR). PCMR is achieved through the addition of a bipolar velocity-encoding gradient to a standard spoiled gradient echo sequence. This bipolar gradient induces an additional phase in moving objects, which is directly proportional to the velocity. Thus, the velocity of an object (i.e. blood) can be calculated using the phase image. Once the velocities are known, it is trivial to estimate volume flow in a region of interest. This technique has been widely validated both *in-vivo* and *in-vitro* and is considered the reference standard method of measuring volume flow. Thus, it has become heavily used in the assessment of cardiac output, cardiovascular shunts and valvar regurgitation. However, PCMR is intrinsically slow because each line in *k*-space must be acquired twice (with different velocity-encodings) in order to perform background phase subtraction. This prolongs the acquisition time and can become extremely problematic in patients in whom several flow maps must be acquired (i.e. congenital heart disease). Consequently, there has been a significant push to accelerate PCMR sequences.

Acceleration techniques

To accelerate CMR, it is necessary to fill *k*-space more quickly. As we have already reached the physical limits of MR gradient systems, this can only be accomplished through undersampling of *k*-space or more efficient filling. Undersampling in *k*-space leads to fold-over artifacts, which makes the data unusable if the artifact overlays the region-of-interest. Parallel imaging techniques (e.g. SENSE or GRAPPA) can be used to reconstruct artifact free images from undersampled data, through the use of independent coil sensitivities. These parallel imaging techniques can significantly speed up 2D PCMR (typically up to 2 times for Cartesian acquisitions. Data undersampling is currently used by most CMR units to speed up the acquisition of flow data. However, the amount of achievable acceleration is limited, leading to studies into alternative techniques for reconstructing artifact free images. The most obvious examples are temporal encoding techniques (e.g. *k-t* BLAST) that can be used alone or in conjunction with parallel imaging techniques (e.g. UNFOLD-SENSE). These techniques offer higher acceleration factors, although often at the cost of some temporal blurring. Currently, these techniques have not become clinically mainstream, however they should further improve workflow when they do.

An additional method of accelerating PCMR is more efficient filling of *k*-space, using a non-Cartesian trajectory. Examples are EPI and spiral *k*-space filling, both of which can significantly speed up acquisition. Furthermore, they can be combined with the previously mentioned techniques to achieve high levels of acceleration. In the next section we will discuss specific uses of acceleration in PCMR.

Rapid cardiac-gated PCMR

PCMR is heavily used in the assessment of conditions such as congenital heart disease, where between 4 to 8 separate flow measurements are often performed. However, particularly in children[1], the accuracy of PCMR is dependent on spatial and temporal resolution. Thus, in this population it is desirable to perform high spatio-temporal resolution flow imaging. Unfortunately because PCMR is intrinsically slow it is difficult to acquire this sort of data in a breath-hold. Hence, cardiac-gated PCMR often relies on multiple signal averages to compensate for respiratory motion, resulting in scan times of approximately 2 minutes. Therefore, complete flow assessment can take around 10 minutes. Thus, in this population there is a need for a high spatio-temporal resolution gated PCMR sequence that can be performed within a short breath-hold.

Previous studies have investigated speeding up Cartesian gated PCMR with the use of SENSE parallel imaging. Beerbaum, et al. [1, 2] showed that undersampling by factors of 2 or 3 did not hamper their ability to measure stroke volumes and pulmonary-to-systemic flow ratios. Lew, et al. [3] were able to show that breath-hold PCMR (acquisition time: 7-10 seconds) was possible if accelerated by SENSE (x3). Thus, parallel imaging can be combined with PCMR to significantly accelerate acquisition.

Even greater acceleration is possible if parallel imaging is combined with efficient *k*-space trajectories. Our group has shown that combining efficient spiral *k*-space filling with SENSE (x3) allows high temporal-spatial resolution PCMR data (Fig. 1) to be acquired in a short breath-hold (6 RR-intervals) [4]. Further-

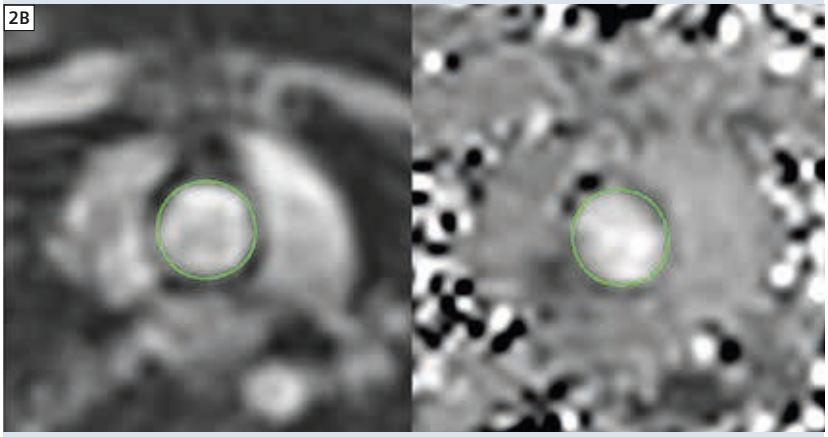

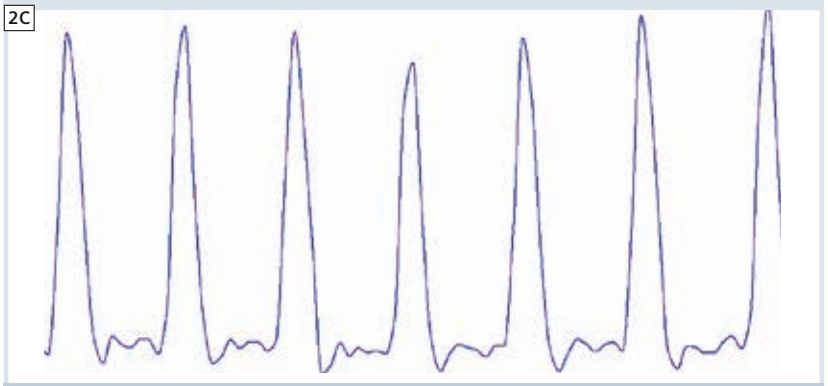

2 Real-time PCMR used for quantification of flow during exercise. **(2A)** MR-compatible ergometer used within the scanner (MR cardiac ergometer Up/Down, Lode, Groningen, Netherlands). **(2B)** Example of image quality achieved using undersampled spiral trajectories in the ascending aorta, left: magnitude, right: phase. **(2C)** Real-time flow curves achieved using this technique.

more, we have shown in a large group of children[1] and adults with congenital heart disease that there were no significant differences compared to a free-breathing Cartesian sequence.
Such sequences allow a reduction in the total duration of flow imaging in congenital heart disease from ~10 minutes, to less than 1 minute. This would lead to a marked reduction in total scan time and has implications for patient throughput and compliance for congenital cardiac MR scanning.
Another approach that has recently become popular is temporal encoding. Baltes, et al. [5] have shown that Cartesian PCMR accelerated with *k-t* BLAST or *k-t* SENSE can lead to significant reductions in scan time. In the future, these temporal encoding techniques could be combined with efficient *k*-space filling strategies to produce very high acceleration factors.

Real-time PCMR

Gated PCMR is the mainstay of clinical flow imaging. However, there are several situations where gated imaging is not suitable, for example, during exercise. Exercise is a powerful stimulator of the cardiovascular system and can be used to unmask subtle disease. However, real-time PCMR is necessary to measure flow during exercise. This can also be achieved through data undersampling and efficient *k*-space filling. For example, Hjortdal, et al. [6] have demonstrated the use of efficient EPI trajectories, with partial-Fourier acquisition, to achieve real-time imaging for the investigation of flow during exercise. This sequence was used to successfully assess exercise hemodynamics in complex congenital heart disease.
Our group has investigated the use of efficient spiral trajectories combined with SENSE (x4) to measure flow at rest and during continuous exercise [7]. The sequence had a high temporal resolution and was validated against a standard gated Cartesian PCMR sequence at

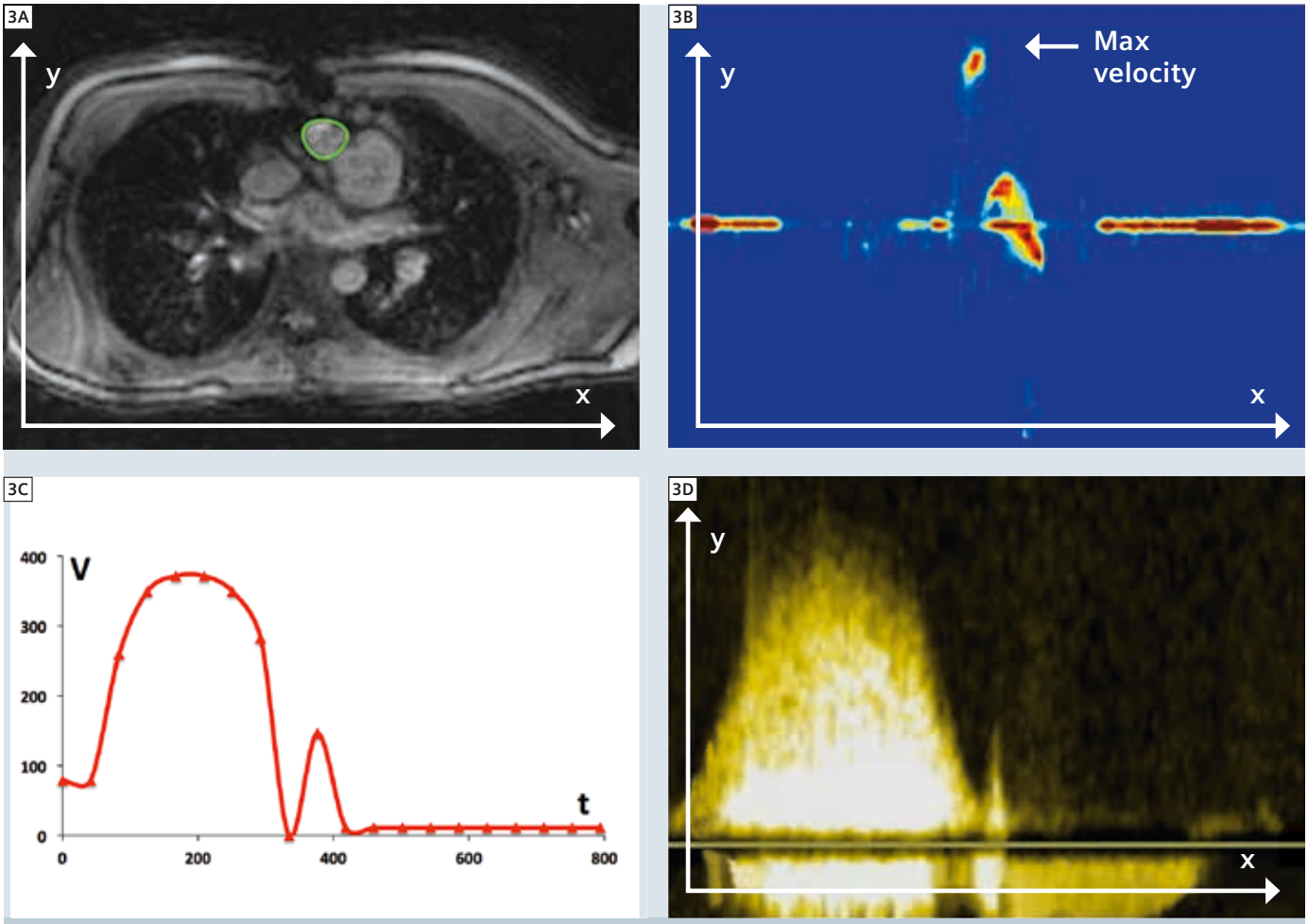

3 Fourier Velocity Encoding using an undersampled spiral acquisition, in one patient. **(3A)** Acquired data in x-y, MIP'd through v. **(3B)** Velocity spectrum along x, at time of peak flow. **(3C)** Velocity profile through time as measured from the spiral MR acquisition. **(3D)** Velocity profile in the same patient as measured using Doppler Ultrasound.

rest, with good agreement (Fig. 2). Using this sequence it was possible to comprehensively assess the response to exercise both in volunteers and patients [8].

Of course, one major problem with this approach is the long reconstruction times associated with non-Cartesian parallel imaging. For example, our group has investigated continuous flow assessment over ~10 minutes during exercise [9]. Using the scanners CPU-based reconstruction, images would only be available ~1 hour after the end of data acquisition. This is too long to be used in a clinical environment; therefore it was necessary to develop a faster reconstruction. One method to achieve this was to use graphical processing unit (GPU)-based reconstruction. This methodology has previously been shown to significantly speed up complex MR reconstructions [10]. In our implementation, a separate GPU-based reconstructor was linked into the scanners reconstruction pipeline, allowing online reconstruction that is hidden from the end-user. Using this technique, images were available ~10 seconds after the end of data acquisition. This type of highly accelerated acquisition and real-time reconstruction may open up many novel areas in cardiovascular MR that are currently impeded by long reconstruction times.

Fourier velocity encoding

Real-time PCMR requires significant acceleration because each frame must be acquired quickly. However, acceleration is also required if large data sets are to be acquired in a short period of time. One good example is Fourier velocity

4

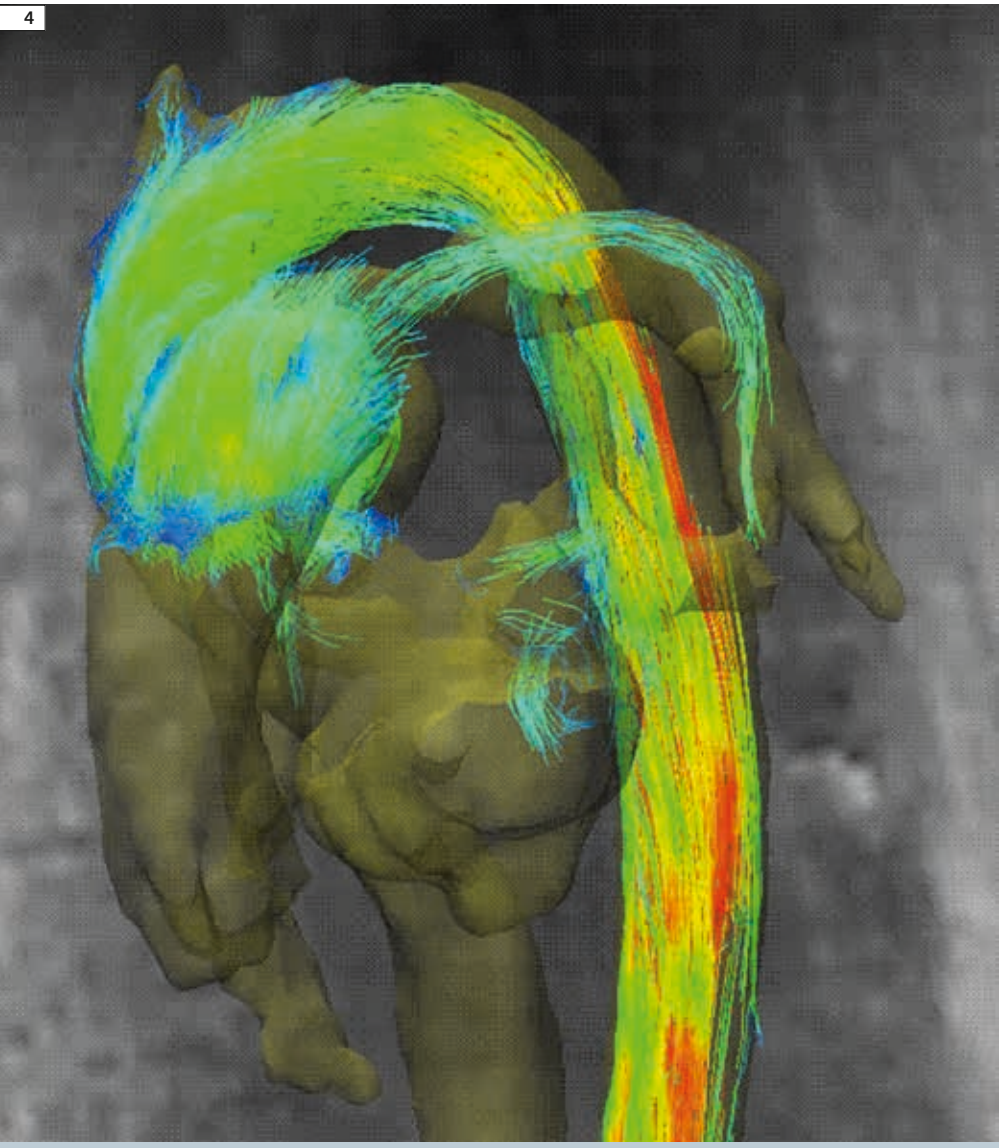

4 4D PCMR data acquired *in-vivo* using an undersampled spiral acquisition.

encoding (FVE), which is a 3D *k*-space acquisition with spatial encoding in two dimensions (*x* and *y*) and velocity encoding in the z direction (denoted as *kv*). Multiple *kv* positions are acquired using bipolar flow-encoding gradients with different first-order moments. Inverse Fourier transformation of *k*-space produces a 3D image with each point in *x-y* space associated with a spectrum of velocities in *v*. This spectrum of velocities allows accurate assessment of stenotic flow, which is often underestimated by traditional PCMR. The main problem with FVE is that it is time consuming to acquire and thus rarely used in the clinical setting.

Time-efficient spiral trajectories with partial-Fourier acquisition along the velocity-encoding dimension have been used to speed up FVE [11]. This form of acceleration does allow breath-hold FVE to be achieved (of 7 RR-intervals), although with a low spatial resolution (of 7 mm). Other groups have investigated the use of *k-t* SENSE for Cartesian FVE [12] with higher acceleration factors (x8 and x16) allowing better spatial resolution (of 1.3-2.8 mm, within a breath-hold of 15-20 seconds).

Our solution to achieve high resolution FVE was to combine spiral trajectories with SENSE in *kx-ky* (x4), in addition to partial-Fourier acquisition in *kv* (67%) and velocity unwrap in the *v* dimension (Fig. 3). The result of all these different acceleration techniques is that it is possible to achieve high spatial (~2.3 mm), temporal (~41 ms) and velocity resolution (14-25 cm/s) FVE data in a relatively short breath-hold (of 15 RR-intervals) [13].

This FVE technique was shown to provide more accurate peak velocity measures than PCMR *in-vitro* and *in-vivo*, compared to Doppler US. Thus, by using acceleration techniques it was possible to bring a technique that has been available for some time, into the clinical environment.

4D Flow

Another technique that has been available for some time, but is rarely used clinically, is time-resolved 3-dimensional PCMR imaging. This technique acquires flow in three encoding directions (known as 4D PCMR) and allows quantification of flow in any imaging plane, in addition to the visualization of complex flow patterns. However, 4D PCMR is rarely used in the clinical setting due to long acquisition times, often in the order of 10-20 minutes.

Several acceleration approaches have been investigated in 4D PCMR. For instance, SENSE and *k-t* BLAST can accelerate the acquisition of Cartesian 4D PCMR at 1.5T and 3T [14]. Using such techniques, it is possible to acquire high-resolution data in ~10 minutes, giving reasonable agreement in terms of stroke

volumes with gated 2D PCMR. Another possibility is the use of combined parallel imaging and compressed-sensing to accelerate the acquisition of 4D PCMR [15]. *K*-space data can be acquired with variable-density Poisson disc undersampling with a total acceleration of 4–5, giving an acquisition time of ~11 minutes.

We have taken a similar approach to FVE and used a stack-of-spirals acquisition in addition to data undersampling, and reconstructing with SENSE to greatly reduce the acquisition time for 4D PCMR. For example, a developed spiral SENSE sequence with 8 uniform density spiral interleaves in *kx-ky*, and 24 slices, can be acquired with a SENSE undersampling factor of 4 in *kx-ky*, and SENSE undersampling factor of 2 in *kz*, giving a total undersampling factor of 8. This allows a temporal resolution of ~49 ms and a spatial resolution of 2.6 × 2.6 × 2.5 mm, to be achieved within a scan time 2 minutes 40 seconds (Fig. 4). In this case, accelerated imaging can offer huge reductions in scan time.

Conclusion and future

Accelerated techniques offer the possibility of significantly speeding up PCMR acquisitions. This should allow better real-time imaging, as well as the acquisition of larger data sets in much shorter times (e.g. 4D PCMR). In the future new acceleration techniques such as compressed sensing may further improve our ability to acquire this sort of data. However, as the acceleration techniques become more complex, faster reconstruction will become necessary. Thus, the advent of GPU based MR reconstruction has a pivotal role to play in the development of new accelerated PCMR sequences.

Contact
Jennifer Steeden
Vascular imaging and physics group
University College London (UCL)
Centre for Cardiovascular Imaging
London
United Kingdom
j.a.steeden@gmail.com

[1] MR scanning has not been established as safe for imaging fetuses and infants under two years of age. The responsible physician must evaluate the benefit of the MRI examination in comparison to other imaging procedures.

References

1 Beerbaum P, Korperich H, Gieseke J, Barth P, Peuster M, Meyer H. Rapid Left-to-Right Shunt Quantification in Children by Phase-Contrast Magnetic Resonance Imaging Combined With Sensitivity Encoding (SENSE). Circ 2003;108(11):1355-1361.

2 Beerbaum P, Körperich H, Gieseke J, Barth P, Peuster M, Meyer H. Blood flow quantification in adults by phase-contrast MRI combined with SENSE--a validation study. Journal of cardiovascular magnetic resonance 2005;7(2):361-369.

3 Lew CD, Alley MT, Bammer R, Spielman DM, Chan FP. Peak Velocity and Flow Quantification Validation for Sensitivity-Encoded Phase-Contrast MR Imaging. Academic Radiology 2007;14(3):258-269.

4 Steeden JA, Atkinson D, Hansen MS, Taylor AM, Muthurangu V. Rapid Flow Assessment of Congenital Heart Disease with High-Spatiotemporal-Resolution Gated Spiral Phase-Contrast MR Imaging. Radiology 2011;260(1):79-87.

5 Baltes C, Kozerke S, Hansen MS, Pruessmann KP, Tsao J, Boesiger P. Accelerating cine phase-contrast flow measurements using *k-t* BLAST and *k-t* SENSE. MRM 2005;54(6):1430-1438.

6 Hjortdal VE, Emmertsen K, Stenbog E, Frund T, Schmidt MR, Kromann O, Sorensen K, Pedersen EM. Effects of Exercise and Respiration on Blood Flow in Total Cavopulmonary Connection: A Real-Time Magnetic Resonance Flow Study. Circ 2003;108(10):1227-1231.

7 Steeden JA, Atkinson D, Taylor AM, Muthurangu V. Assessing vascular response to exercise using a combination of real-time spiral phase contrast MR and noninvasive blood pressure measurements. Journal of Magnetic Resonance Imaging 2010;31(4):997-1003.

8 McKee A, Davies J, Bilton D, Taylor A, Gatzoulis M, Aurora P, Muthurangu V, Balfour-Lynn I. A Novel Exercise Test Demonstrates Reduced Stroke Volume Augmentation But No Evidence Of Pulmonary Hypertension In Patients With Advanced Cystic Fibrosis. Pediatr Pulm 2011:354.

9 Kowalik GT, Steeden JA, Pandya B, Odille F, Atkinson D, Taylor A, Muthurangu V. Real-time flow with fast GPU reconstruction for continuous assessment of cardiac output. Journal of Magnetic Resonance Imaging 2012;36(6): 1477-1482.

10 Hansen MS, Atkinson D, Sorensen TS. Cartesian SENSE and *k-t* SENSE reconstruction using commodity graphics hardware. MRM 2008;59(3):463-468.

11 Carvalho JLA, Nayak KS. Rapid quantitation of cardiovascular flow using slice-selective fourier velocity encoding with spiral readouts. MRM 2007;57(4):639-646.

12 Baltes C, Hansen MS, Tsao J, Kozerke S, Rezavi R, Pedersen EM, Boesiger P. Determination of Peak Velocity in Stenotic Areas: Echocardiography versus kt SENSE Accelerated MR Fourier Velocity Encoding. Radiology 2007;246(1):249.

13 Steeden JA, Jones A, Pandya B, Atkinson D, Taylor AM, Muthurangu V. High-resolution slice-selective Fourier velocity encoding in congenital heart disease using spiral SENSE with velocity unwrap. MRM 2012;67(6):1538-1546.

14 Carlsson M, Toger J, Kanski M, Bloch K, Stahlberg F, Heiberg E, Arheden H. Quantification and visualization of cardiovascular 4D velocity mapping accelerated with parallel imaging or *k-t* BLAST: head to head comparison and validation at 1.5 T and 3 T. Journal of Cardiovascular Magnetic Resonance 2011;13(1):55.

15 Tariq U, Hsiao A, Alley M, Zhang T, Lustig M, Vasanawala SS. Venous and arterial flow quantification are equally accurate and precise with parallel imaging compressed sensing 4D phase contrast MRI. Journal of Magnetic Resonance Imaging 2012:n/a-n/a.

Free-Breathing Real-Time Flow Imaging using EPI and Shared Velocity Encoding

Ning Jin[1]; Orlando Simonetti, Ph.D.[2]

[1]Siemens Healthcare, Malvern, PA, USA
[2]The Ohio State University, Columbus, OH, USA

Introduction

Phase-contrast magnetic resonance imaging (PC-MRI) is used routinely as an important diagnostic tool to measure blood flow and peak velocities in major blood vessels and across heart valves. Conventional PC-MRI commonly uses ECG synchronization and segmented *k*-space acquisition strategies [1, 2]; this approach requires breath-holding and regular cardiac rhythm, rendering it impractical in a large number of patients. Alternatively, signal averaging and respiratory gating approaches can be used to reduce respiratory motion artifacts in patients unable to breath-hold, but these methods still require a reliable ECG signal and regular heart beats. Furthermore, the velocity information resulting from an ECG-synchronized segmented PC sequence represents a weighted temporal average of the velocity waveform over the acquisition time; short-lived hemodynamic effects, such as response to pharmacological stress, physical exercise or respiration and interventional maneuvers cannot be assessed. Hence, free-breathing real-time (RT) PC-MRI with sufficient spatial/temporal resolution would be desirable to provide beat-to-beat hemodynamic information to characterize transient blood flow phenomena and as an alternative approach for patients with irregular cardiac rhythm or inability to hold their breath.

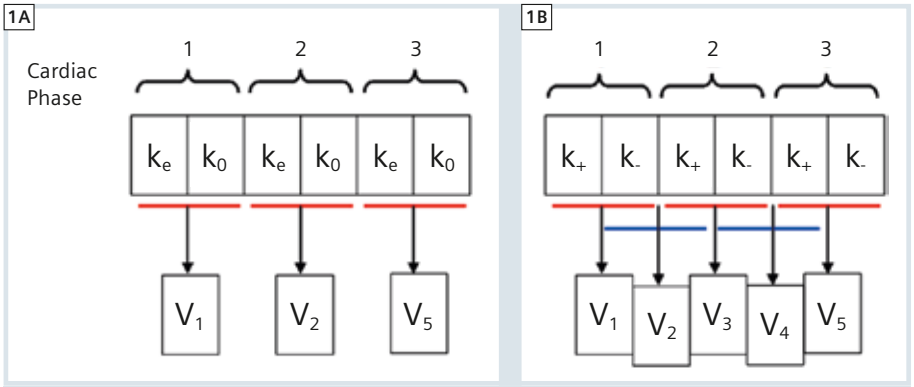

1 **(1A)** The conventional PC with 1-sided velocity encoding. Velocity information was extracted using the flow encoded (k_e) and flow compensated (k_0) data within the same cardiac phase. **(1B)** SVE with 2-sided velocity encoding. Additional velocity frames (V_2 and V_4) are reconstructed by sharing the flow encoded data across cardiac phases to double the effective frame rate by a factor of 2.

Methods

RT PC-MRI sequence was implemented using a gradient-echo echo-planar imaging (GRE-EPI) sampling trajectory with an echo train length (ETL) of 7 to 15 echoes. A rapid phase modulated binomial spatial and spectral selective water excitation pulse was used to eliminate ghosting artifacts from fat tissue. Temporal parallel acquisition technique (TPAT) with an acceleration factor of 3 was used by temporally interleaving undersampled *k*-space lines [3, 4]. Four shots per image were acquired resulting in an acquisition time about 40 to 50 ms (depending on ETL and matrix size) for each full *k*-space dataset per flow encoding step. To further improve the effective temporal resolution of RT-PC, a shared velocity encoding (SVE) [5] scheme was implemented.

In PC-MRI, a critical step is the elimination of background phase errors. This is achieved by subtracting two measurements with different flow encodings. It is typically performed using one of two methods: one-sided velocity encoding in which velocity compensated (k_0) and velocity encoded (k_e) data are acquired for each cardiac phase, or two-sided velocity encoding in which equal and opposite velocity encodings (k_+/k_-) are acquired. Both cases result in a reduc-

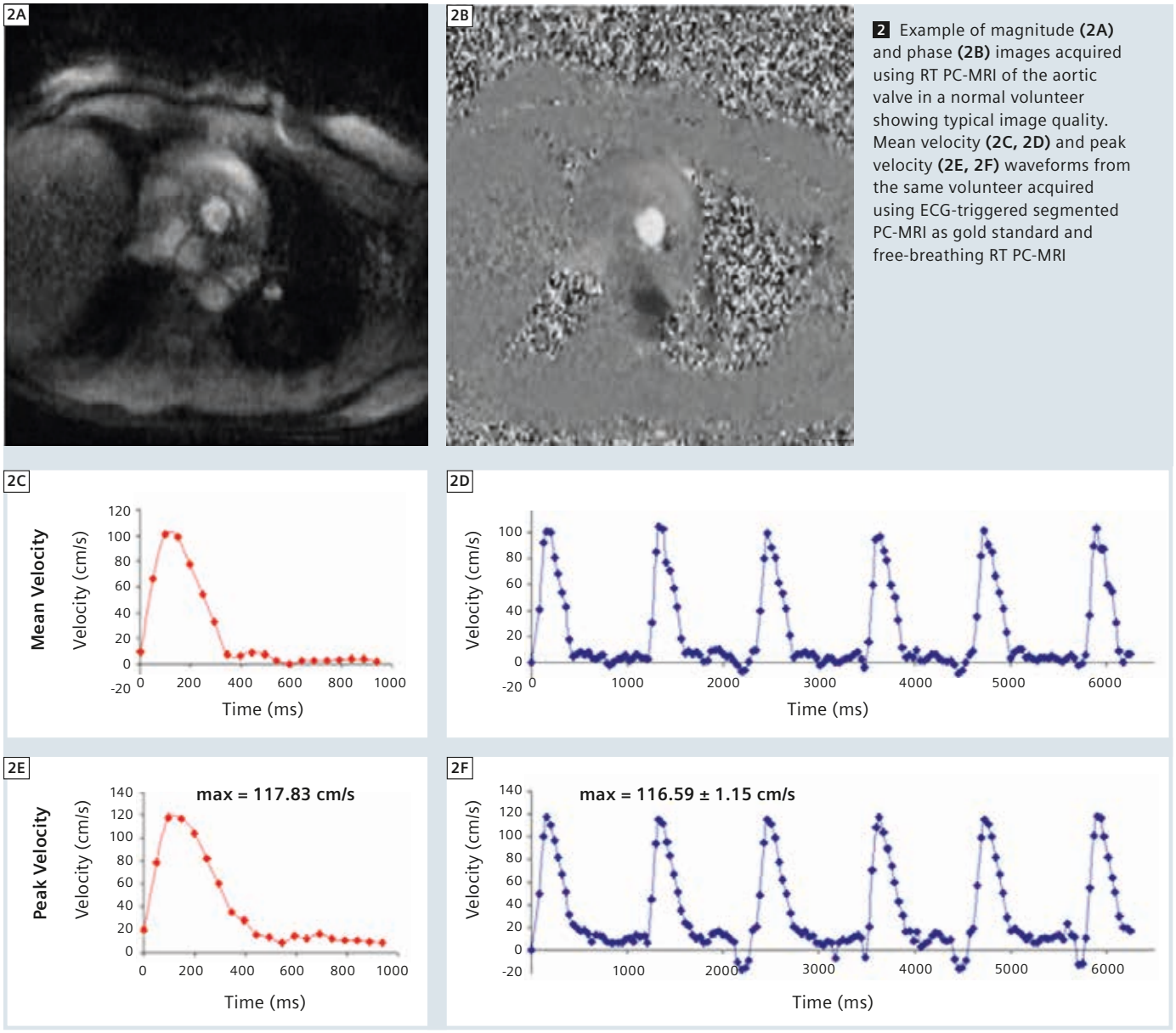

2 Example of magnitude **(2A)** and phase **(2B)** images acquired using RT PC-MRI of the aortic valve in a normal volunteer showing typical image quality. Mean velocity **(2C, 2D)** and peak velocity **(2E, 2F)** waveforms from the same volunteer acquired using ECG-triggered segmented PC-MRI as gold standard and free-breathing RT PC-MRI

tion in temporal resolution or an increase in scan time by a factor of two. The SVE concept is to share flow encoded data between two adjacent frames in a two-sided velocity encoded PC-MRI. Figure 1 illustrates the difference between conventional PC reconstruction with one-sided velocity encoding and SVE reconstruction with two-sided velocity encoding. The odd-number velocity frames (V1, V3 and V5) are identical to the frames generated by the conventional PC reconstruction, while SVE reconstruction results in the intermediate even frames 2 and 4. While each of these additional frames shares velocity data with the adjacent frames, each contains a unique set of data that represents a velocity measurement centered at the time between the original frames. As the result, SVE increases the effective temporal resolution by a factor of two. While the SVE method doubles the effective frame rate; the temporal window of each frame is unchanged. In the RT-PC works-in-progress (WIP) sequence, the effective, reconstructed temporal resolution of each frame is 40 to 50 ms while the temporal window to acquire all flow encoding steps is 80 to 90 ms.

Results

Figure 2 shows the representative magnitude (Fig. 2A) and phase (Fig. 2B) images and the velocity waveforms of the aortic valve in one normal volunteer acquired using ECG-triggered segmented PC-MRI in breath-hold (Figs. 2C and 2E) and RT PC-MRI in free-breathing (Figs. 2D and 2F). The results from ECG-triggered segmented PC-MRI are used as the reference standard. The mean velocity

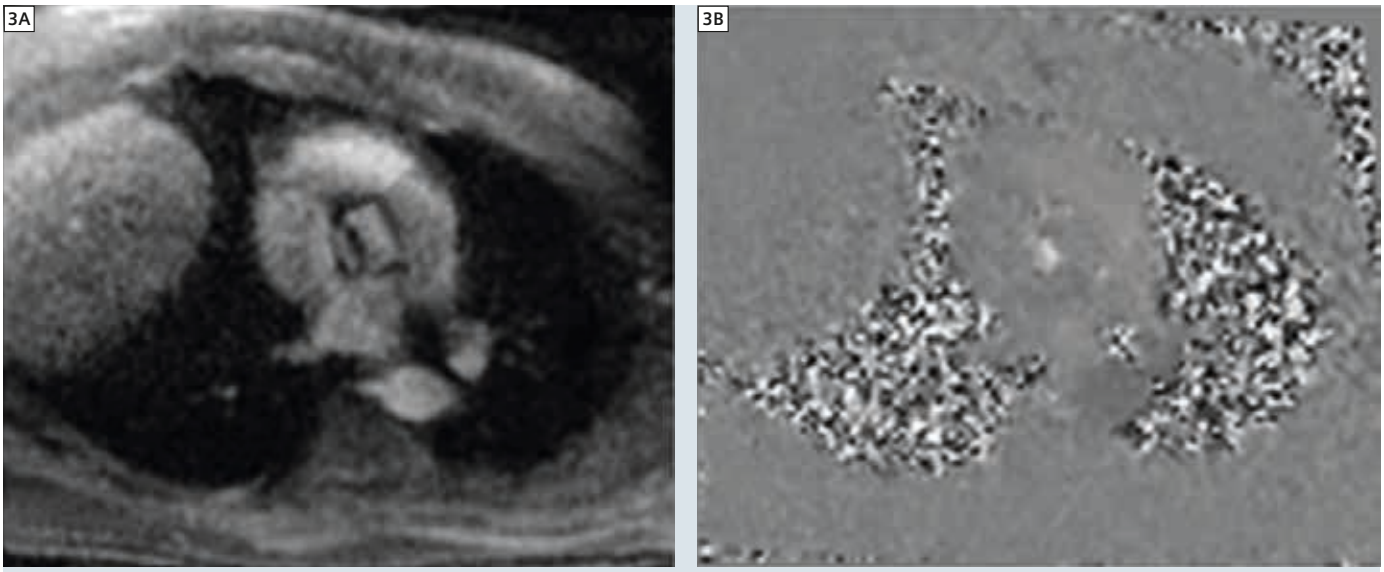

3 Magnitude **(3A)** and phase **(3B)** images acquired using RT PC-MRI of the aortic valve in one patient with bicuspid aortic valve and moderate aortic stenosis.

curve (Fig. 2D) and the peak velocity curve (Fig. 2F) acquired using RT PC-MRI match well with those of the reference standard (Figs. 2C and 2E). The maximum peak velocity from RT-MRI is 116.59 ± 1.15 cm/s averaged over six heart beats, which agrees well with the reference standard (117.83 cm/s). Figure 3 shows the magnitude and phase images of the aortic valve acquired with RT PC-MRI in one patient with bicuspid aortic valve and moderate aortic stenosis. RT PC-MRI measured a peak velocity of 330 cm/s and planimetered valve area of 1.2 cm^2.

Conclusion

We have described a free-breathing RT PC-MRI technique that employs a GRE-EPI sampling trajectory, TPAT acceleration and SVE velocity encoding scheme. It is a promising approach for rapid and RT flow imaging and measurements. The technique has been shown to provide accurate blood flow measurements with sufficient SNR and spatial/temporal resolution [5]. With RT EPI acquisition, the adverse effects of cardiac and respiratory motion on flow measurements are minimized. Thus, RT PC-MRI can be used on patients suffering from arrhythmia, and in pediatric or other patients incapable of breath-holding. Furthermore, RT PC-MRI provides transient hemodynamic information, which could be used to evaluate the effects of respiration, exercise, or other physical maneuvers on blood flow [6].

Contact
Orlando "Lon" Simonetti, Ph.D.
Professor of Internal Medicine and Radiology
The Ohio State University
460 W. 12th Ave., BRT316
Columbus, OH 43210
Phone: +1 (614) 293-0739
Fax: +1 (614) 247-8277
Orlando.Simonetti@osumc.edu

References
1 Chatzimavroudis GP et al. Clinical blood flow quantification with segmented *k*-space magnetic resonance phase velocity mapping. J Magn Reson Imaging 2003;17:65–71.
2 Edelman RR et al. Flow velocity quantification in human coronary arteries with fast, breath-hold MR angiography. J Magn Reson Imaging 1993;3:699–703.
3 Kellman P et al. Adaptive Sensitivity Encoding Incorporating Temporal Filtering (TSENSE). Magn Reson Med. 45: 846-852 (2001).
4 Breuer FA et al. Dynamic autocalibrated parallel imaging using temporal GRAPPA (TGRAPPA). Magn Reson Med. 53(4): 981-985 (2005).
5 Lin HY et al. Shared velocity encoding: a method to improve the temporal resolution of phase-contrast velocity measurements, Magn Reson Med 2012;68:703–710
6 Thavendiranathan et al., Simultaneous right and left heart real-time, free-breathing CMR flow quantification identifies constrictive physiology. JACC Cardiovasc Imaging. 2012 Jan;5(1):15-24.

High Acceleration Quiescent-Interval Single Shot Magnetic Resonance Angiography at 1.5 and 3T

Maria Carr R.T.R (CT)(MR)[1]; Christopher Glielmi, Ph.D.[2]; Robert R. Edelman, M.D.[3]; Michael Markl, Ph.D.[1]; James Carr, M.D.[1]; Jeremy Collins, M.D.[1]

[1]Northwestern Memorial Hospital and Northwestern University Feinberg School of Medicine, Chicago, IL, USA
[2]Cardiovascular MR R&D, Siemens Healthcare, Chicago, IL, USA
[3]NorthShore University HealthSystem, Evanston, IL, USA

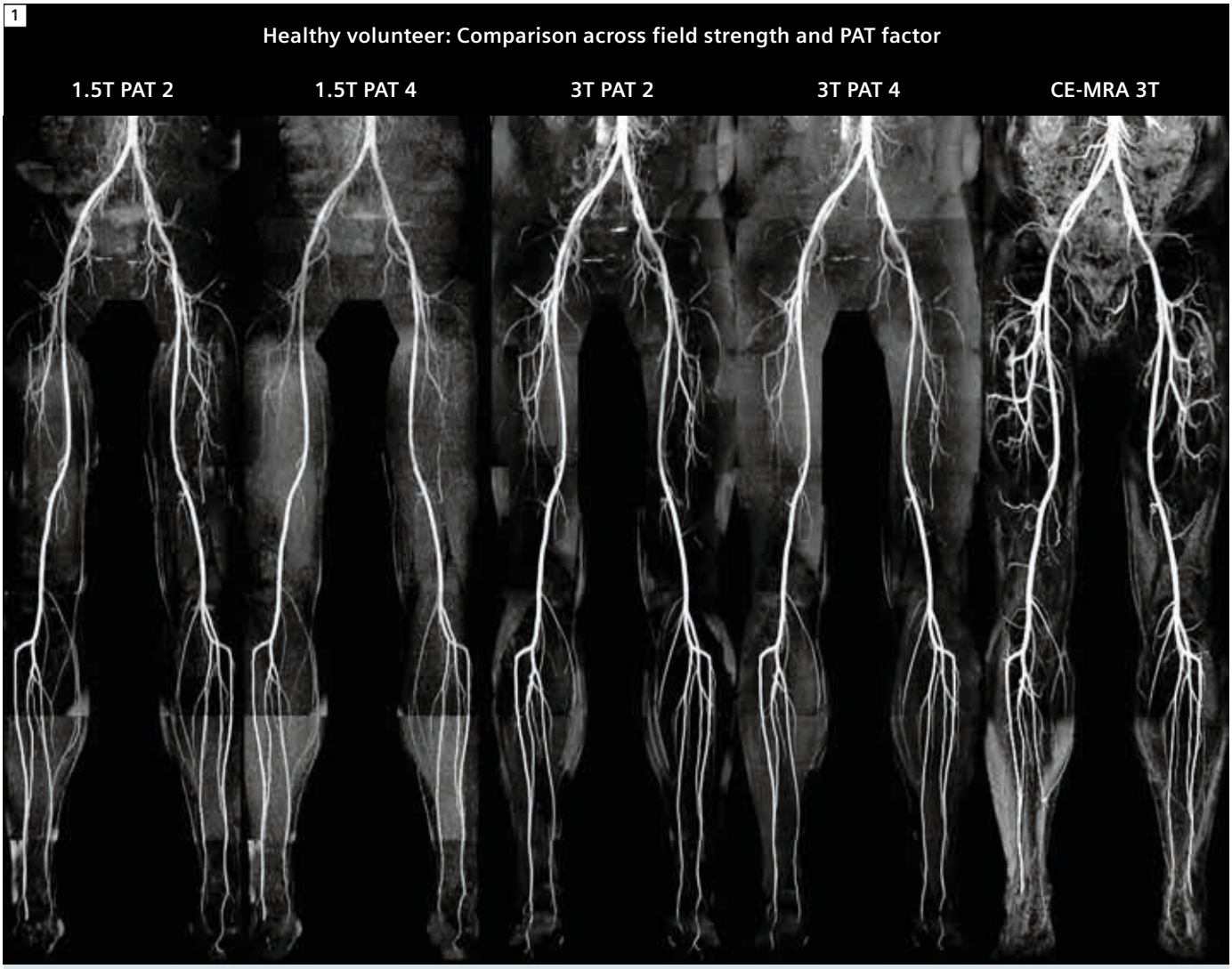

1 QISS maintains excellent image quality with PAT 4 acquisition. 3T imaging demonstrates higher SNR and potentially better results at high PAT factors. All protocols have high correlation to CE-MRA (right).

Background

Contrast-enhanced MR angiography (CE-MRA) is routinely used for the evaluation of peripheral arterial disease (PAD). However, due to the increased concern of nephrogenic systemic fibrosis (NSF) associated with gadolinium administration in patients with impaired renal function, there has been increased interest in the development of non-contrast MRA (NC-MRA) techniques. Quiescent-interval single-shot (QISS) imaging* has recently been described as an NC-MRA technique for assessment of the lower extremity vasculature [1] with proven clinical utility at 1.5T [2, 3]. These studies have demonstrated that QISS is easy to use, does not require patient-specific imaging parameters, has minimal flow dependence and is less sensitive to motion than subtractive techniques. Increased SNR at 3T potentially provides improved image quality and enable higher parallel imaging acceleration (PAT) factors. Increasing the PAT factor can be critical to maintaining an acquisition rate of one slice per heartbeat in patients with fast heart rates. In order to evaluate these aspects of QISS NC-MRA, the purpose of our study was to determine

1. the effect of field strength on QISS image quality,
2. the potential to accelerate imaging at 3T using higher PAT factors and
3. to compare NC-MRA QISS at 3T to a conventional CE-MRA protocol.
   In addition, the diagnostic quality of QISS at 3T in patients with PAD was evaluated.

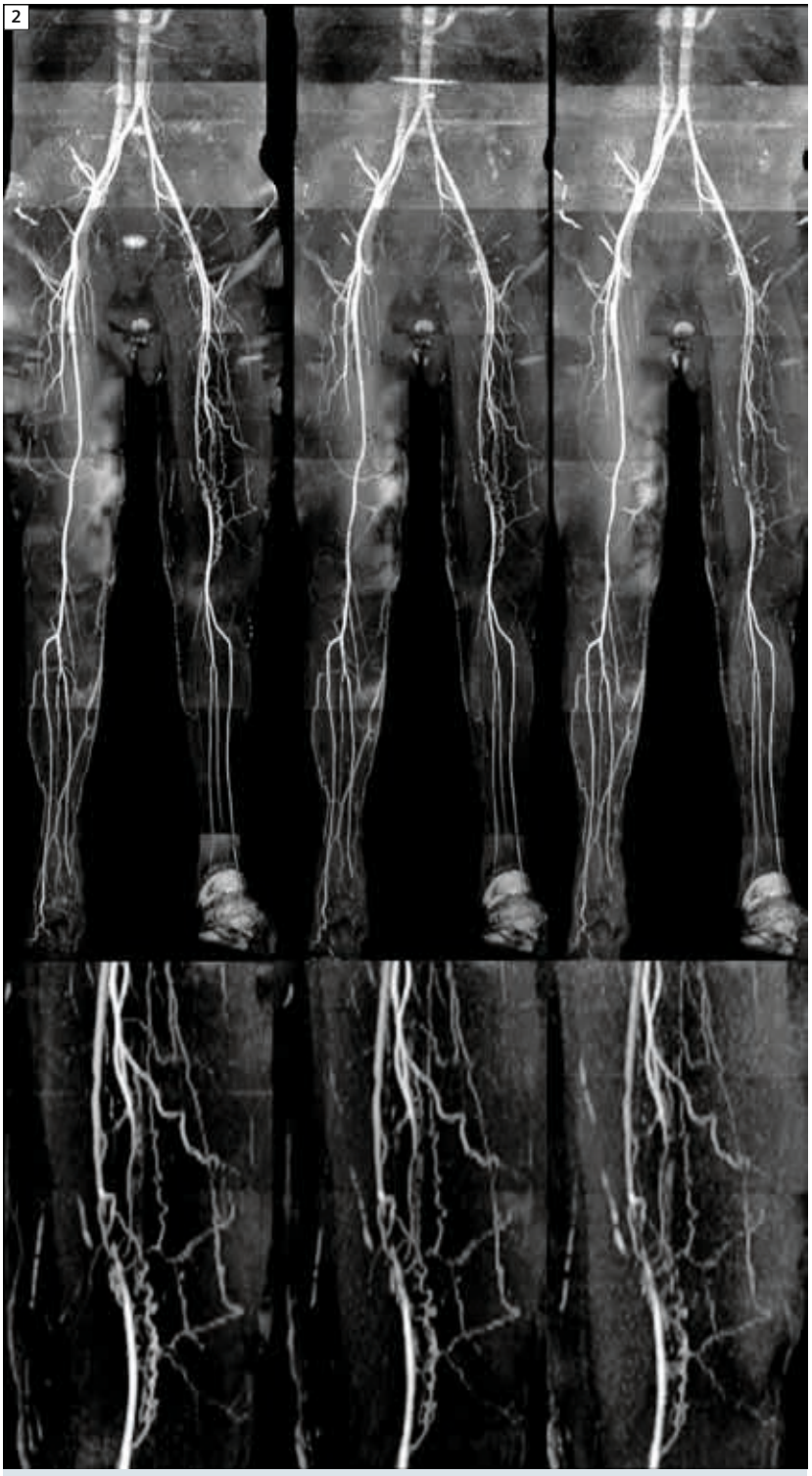

2 3T QISS in a patient shows segmental occlusion in the adductor canal with reconstitution in the profunda femoral collateral for patient with low GFR (no CE-MRA reference). Standard PAT factor 2 (left), as well as higher PAT factors 3 (center) and 4 (right) clearly depict disease, enabling shorter single shot acquisition capabilities for patients with fast heart rates.

Reprinted from MAGNETOM Flash 1/2012.

Methods

QISS is a two-dimensional electrocardiographically gated single-shot balanced steady-state free precession acquisition of one axial slice per heartbeat. Image contrast is generated using in-plane saturation to suppress background tissue and a tracking saturation pulse to suppress venous signal prior to a quiescent inflow period. ECG gating ensures that the quiescent inflow period coincides with rapid systolic flow to maximize inflow of unsaturated spins into the imaging slice; since only a 2D slice is saturated, only minimal inflow is required. Images are acquired with a series of imaging stations, each with 70 slices around the magnet isocenter. Stations in the pelvis and abdomen typically use a series of breath-hold concatenations to minimize respiratory motion.

To validate QISS at 3T, twelve healthy volunteers (9 males age 22–49, 3 females age 26–43) were scanned at 1.5 and 3T within one week using a dedicated 36-channel peripheral vascular coil and an 18-channel body array coil (1.5T MAGNETOM Aera and 3T MAGNETOM Skyra, Siemens Healthcare, Erlangen, Germany). In addition, CE-MRA was performed at 3T (8.4–10 ml at 2 ml/sec, Ablavar, Lantheus Medical Imaging, N. Billerica, MA, USA). Additionally, 3 patients with lower extremity PAD were scanned using 3T QISS NC-MRA and CE-MRA as the reference standard if glomerular filtration rate (GFR) was sufficient. Imaging parameters are provided in Table 1. For each scan session, three QISS run-off scans were acquired in randomized order with GRAPPA PAT factors 2, 3 and 4. The total acquisition and shim time for each QISS NC-MRA run-off was approximately 10 minutes depending on the heart rate. Two blinded radiologists scored image quality for venous contamination, arterial conspicuity and arterial artifacts using a 4-point scale (0 = poor, 1 = fair, 2 = good, 3 = excellent) and inter-observer reliability was measured using the kappa statistic.

Validation results

QISS image quality was consistent for both field strengths. 3T results were particularly robust, even with high PAT factors and showed higher signal-to-noise ratio (SNR) relative to 1.5T (representative volunteer in Fig. 1). Arterial conspicuity and artifact scores were comparable to CE-MRA, and slightly higher for 3T (2.8 ± 0.1) relative to 1.5T (2.5 ± 0.2). Venous suppression was superior at 1.5T; venous signal did not impact arterial assessment at 3T, however. QISS at 3T also had higher inter-observer agreement ($\kappa = 0.759$) than at 1.5T ($\kappa = 0.426$) for image quality scoring. Overall, QISS performed comparably to CE-MRA at both field strengths, even with a high PAT factor of 4 [4]. Despite the presence of respiratory or bowel motion in some volunteers, QISS with concatenated breath-holding performed consistently in the abdomen and pelvis. Moreover, one always has the option to repeat all or part of the data acquisition in case of technical difficulty or macroscopic patient motion - an option that is not afforded by CE-MRA.

Clinical results

Based on impressive results in volunteers, several patients were scanned at 3T to demonstrate clinical utility. Initial results suggest that QISS is effective at 3T and has high correlation with CE-MRA.

Clinical case 1

42-year-old male with longstanding history of type I diabetes complicated by renal failure presents with left diabetic foot requiring transmetatarsal amputation. He subsequently received a kidney transplant and now presents to vascular surgery clinic with non-healing wounds of the right 3rd and 4th toes. The patient's renal function is poor, with a Creatinine of 2.35 mg/dl and an eGFR of 31 ml/min/1.73 m^2. The patient was referred for QISS NC-MRA at 3T to assess options for right lower extremity revascularization (Fig. 2). NC-MRA demonstrated segmental occlusion of the distal left superficial femoral artery at the adductor canal over a distance of approximately 3 cm with reconstitution via branches of the profunda femoris artery (Fig. 2). Small collateral vessels are clearly depicted for PAT factors 2, 3, and 4 (suitable for 738, 660 and 619 ms R-R intervals, respectively) suggesting that high PAT factors can be used to maintain acquisition of one slice per heartbeat for patients with high heart rates. The QISS NC-MRA images of the calves clearly depict the arterial run-off beyond the level of occlusion. No significant arterial stenoses were apparent in the right lower extremity and the patient was diagnosed with microvascular disease. The patient continued wound care, with plans for transmetatarsal amputation if conservative therapy was unsuccessful.

Clinical case 2

64-year-old male with a history of hypertension, chronic back pain, and tobacco abuse presents with diminished exercise tolerance. The patient reports that these symptoms have been slowly progressive over two years such that he is only able to walk half a block, limited by fatigue and left leg weakness of the hip and buttock. Lower extremity arterial flow studies demonstrated an ankle brachial index of 0.69 with duplex findings suggestive of inflow disease. The patient was referred for CE-MRA at 1.5T and underwent QISS NC-MRA at 3T for research purposes (Fig. 3). CE-MRA with a single dose of gadobenate dimeglumine (Multihance, Bracco Diagnostics Inc., Princeton, NJ, USA) demonstrated long segment occlusion of the left external iliac artery, with reconstitution of the common femoral artery. There was no significant left lower extremity outflow disease; three-vessel runoff was noted to the left foot. QISS NC-MRA demonstrated similar findings, with segmental occlusion of the external iliac artery, with the common femoral artery reconstituted by the inferior epi-

gastric and deep circumflex iliac arteries. The patient will undergo revascularization with left iliac stent placement at a later date.

Clinical case 3
56-year-old female with a history of hypertension, type II diabetes, and lumber radiculopathy presents with intermittent left lower extremity claudication gradually increasing in severity over the course of a year, now limiting her walking to a half block. The patient describes increased sensitivity to her left foot and pain in the anterior left thigh, which keeps her awake at night. She notes improved pain with Vicodin. The patient was referred for CE-MRA and underwent QISS NC-MRA at 3T for research purposes (Fig. 4). CE-MRA was performed at 1.5T following a double-dose of gadopentetate dimeglumine (Magnevist, Bayer Healthcare Pharmaceuticals, Inc, Wayne, NJ, USA) demonstrating long segment occlusion of the left mid to distal superficial femoral artery, with reconstitution of the popliteal artery via branches of the hypertrophied profunda femoris artery. These findings are well seen using QISS NC-MRA, which delineates the length of the occlusion and the run-off vessels without contrast media. Mild venous signal contamination is noted on QISS

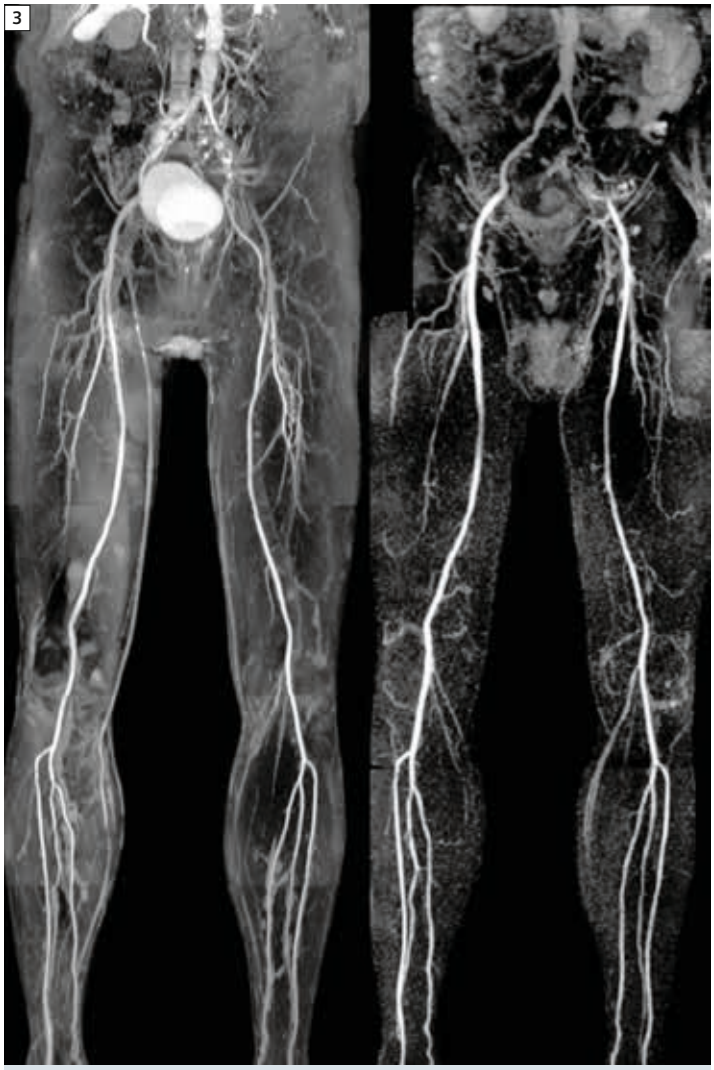

3 Both QISS and CE-MRA depict long segment occlusion of the left external iliac artery, with reconstitution of the common femoral artery. QISS PAT 3 acquisition (left) maximizes SNR while still maintaining single shot acquisition every heartbeat.

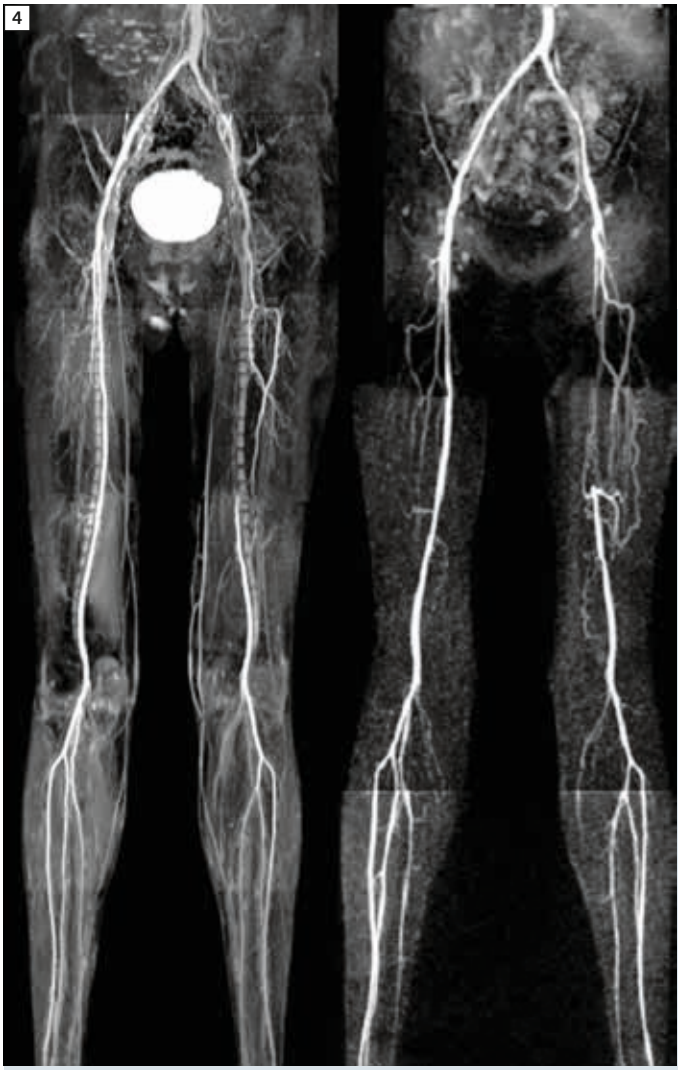

4 QISS and CE-MRA demonstrate long segment occlusion of the left mid to distal superficial femoral artery, with reconstitution of the popliteal artery via branches of the hypertrophied profunda femoris artery. For this patient, QISS PAT 4 acquisition (left) maintained single shot acquisition every heart beat.

Reprinted from MAGNETOM Flash 1/2012.

NC-MRA without impacting diagnostic yield of the maximum intensity projection (MIP) images. The patient underwent successful endovascular recanalization of the left superficial femoral artery with stent placement with resolution of her claudication symptoms.

Conclusion

QISS NC-MRA is promising at 3T and demonstrates comparable image quality to CE-MRA in depicting the peripheral arteries in both volunteers and patients with PAD. Improved SNR at 3T enables higher PAT factors to reduce image acquisition time while maintaining image quality in patients with faster heart rates. While QISS at 1.5T has shown excellent clinical utility, our results suggest that imaging at 3T may provide further clinical benefit. QISS NC-MRA at 3T demonstrated arterial vessels with slightly greater conspicuity and lower arterial artifacts compared to QISS NC-MRA at 1.5T. Although venous signal contamination is greater at 3T, the increased arterial signal enables ready differentiation on MIP imaging and does not impact diagnostic utility. Volunteer and patient data demonstrate that the QISS acquisition can be accelerated up to four fold without significant image quality degradation, suitable for heart rates approaching 100 beats per minute. At both field strengths, the QISS technique is a valuable alternative to CE-MRA especially in patients with renal insufficiency.

Table 1: Quiescent-interval single-shot (QISS) sequence details.

QISS sequence details	
TR (ms) / TE (ms) / flip angle (deg.)	3.2/1.7/90
In-plane resolution	1 x 1 mm
Partial Fourier	5/8
Slice thickness	3 mm
Orientation	axial
No. of slices per group	70
No. of slice groups	7
Acquisition time / slice group	~55 s (heart rate dependent)
Parallel imaging	GRAPPA x 2–4
ECG gating	Yes
Inversion time	345 ms

References

1 Edelman, R.R., et al., Quiescent-interval single-shot unenhanced magnetic resonance angiography of peripheral vascular disease: Technical considerations and clinical feasibility. Magn Reson Med, 2010. 63(4): p. 951–8.

2 Hodnett, P.A., et al., Evaluation of peripheral arterial disease with nonenhanced quiescent-interval single-shot MR angiography. Radiology, 2011. 260(1): p. 282–93.

3 Hodnett, PA, et al., Peripheral Arterial Disease in a Symptomatic Diabetic Population: Prospective Comparison of Rapid Unenhanced MR Angiography (MRA) With Contrast-Enhanced MRA. AJR December 2011 197(6): p. 1466–73.

4 Glielmi, C., et al. High Acceleration Quiescent-Interval Single Shot Magnetic Resonance Angiography at 1.5 and 3T. ISMRM 2012, 3876.

Contact
Maria Carr, RT (CT)(MR)
CV Research Technologist
Department of Radiology
Northwestern University
Feinberg School of Medicine
737 N. Michigan Ave. Suite 1600
Chicago, IL 60611
USA
Phone: +1 312-503-1417
m-carr@northwestern.edu

Global Siemens Headquarters

Siemens AG
Wittelsbacherplatz 2
80333 Muenchen
Germany

Global Siemens Healthcare Headquarters

Siemens AG
Healthcare Sector
Henkestrasse 127
91052 Erlangen
Germany
Phone: +49 9131 84-0
www.siemens.com/healthcare

www.siemens.com/healthcare-magazine

Order No. A91MR-1000-95C-7600 | Printed in Germany | CC 908 01131. | © 01.13, Siemens AG

MAGNETOM Flash – Imprint

Publisher:
Siemens AG
Medical Solutions
Business Unit Magnetic Resonance,
Karl-Schall-Straße 6, D-91052 Erlangen,
Germany

Editor-in-Chief: Milind Dhamankar, M.D.
(milind.dhamankar@siemens.com)

Associate Editor: Antje Hellwich
(antje.hellwich@siemens.com)

Editorial Board: Lars Drüppel, Ph.D.;
Sven Zühlsdorff, Ph.D.; Wellesley Were;
Ralph Strecker; Gary R. McNeal;
Peter Kreisler, Ph.D.; Dr. Sunil Kumar

Production: Norbert Moser, Siemens AG,
Medical Solutions, Erlangen, Germany

Layout: independent Medien-Design
Widenmayerstrasse 16, D-80538 Munich,
Germany

Note in accordance with § 33 Para.1 of the German Federal Data Protection Law: Despatch is made using an address file which is maintained with the aid of an automated data processing system. MAGNETOM Flash with a total circulation of 35,000 copies is sent free of charge to Siemens MR customers, qualified physicians, technologists, physicists and radiology departments throughout the world. It includes reports in the English language on magnetic resonance: diagnostic and therapeutic methods and their application as well as results and experience gained with corresponding systems and solutions. It introduces from case to case new principles and procedures and discusses their clinical potential. The statements and views of the authors in the individual contributions do not necessarily reflect the opinion of the publisher.

We welcome your questions and comments about the editorial content of MAGNETOM Flash. Please contact us at magnetomworld.med@siemens.com.

Manuscripts as well as suggestions, proposals and information are always welcome; they are carefully examined and submitted to the editorial board for attention. MAGNETOM Flash is not responsible for loss, damage, or any other injury to unsolicited manuscripts or other materials. We reserve the right to edit for clarity, accuracy, and space. Include your name, address, and phone numberand send to the editors, address above.

Not for distribution in the US

On account of certain regional limitations of sales rights and service availability, we cannot guarantee that all products included in this brochure are available through the Siemens sales organization worldwide. Availability and packaging may vary by country and is subject to change without prior notice. Some/All of the features and products described herein may not be available in the United States.

The information in this document contains general technical descriptions of specifications and options as well as standard and optional features which do not always have to be present in individual cases.

Siemens reserves the right to modify the design, packaging, specifications and options described herein without prior notice.
Please contact your local Siemens sales representative for the most current information.

Note: Any technical data contained in this document may vary within defined tolerances. Original images always lose a certain amount of detail when reproduced.

Global Business Unit

Siemens AG
Medical Solutions
Magnetic Resonance
Henkestr. 127
DE-91052 Erlangen
Germany
Phone: +49 9131 84-0
www.siemens.com/healthcare

Local Contact Information

Asia
Siemens Pte Ltd
The Siemens Center
60 MacPherson Road
Singapore 348615
Phone: +65 6490-8096

Canada
Siemens Canada Limited
Medical Solutions
2185 Derry Road West
Mississauga ON L5N 7A6
Canada
Phone: +1 905 819-5800

Europe/Africa/Middle East
Siemens AG
Medical Solutions
Henkestr. 127
91052 Erlangen
Germany
Phone: +49 9131 84-0

Latin America
Siemens S.A.
Medical Solutions
Avenida de Pte. Julio A. Roca No 516,
Piso 7
C1067ABN Buenos Aires
Argentina
Phone: +54 11 4340-8400